Journal of Structural Geology 139 (2020) 104147

Contents lists available at ScienceDirect

Journal of Structural Geology

journal homepage: http://www.elsevier.com/locate/jsg

Morphotectonic and earthquake data analysis of interactional faults in Sabzevaran Area, SE Iran

Ahmad Rashidi [a,*], Mohammad-Reza Abbassi [a], Faramarz Nilfouroushan [b,c], Shahram Shafiei [d], Reza Derakhshani [d,e], Majid Nemati [f]

[a] International Institute of Earthquake Engineering and Seismology, Tehran, Iran
[b] Department of Industrial Development, IT and Land Management, University of Gävle, Gävle, Sweden
[c] Department of Geodetic Infrastructure, Geodata Division, Lantmäteriet, Gävle, Sweden
[d] Department of Geology, Shahid Bahonar University of Kerman, Kerman, Iran
[e] Department of Earth Sciences, Utrecht University, Utrecht, the Netherlands
[f] Department of Geology, Faculty of Science and Earthquake Research Center of Shahid Bahonar University of Kerman, Iran

ARTICLE INFO

Keywords:
Active faulting
Fault interaction
Morphotectonics
Sabzevaran area
Iran

ABSTRACT

We used satellite images, earthquake catalogues and field observations to study several active fault systems and their interactions in Sabzevaran Area in SE Iran. The focus of this study is to verify the link between the active faults, their kinematics and seismic activity. Field observations and geomorphological analysis highlight the interaction of the active faults. Moreover, most of the tectonic activity is observed in the area, related to the Chahmazrae- North Faryab shear zone. Most of the earthquakes in this shear zone are reverse and occur in the deeper crust while aftershocks dominantly occur in the shallower crust. The Main Zagros Reverse Fault (MZRF) is the source of reverse events and the Chahmazrae-North Faryab shear zone is source of left-lateral, oblique reverse faulting events, and strike-slip events. These types of the earthquakes in the study area confirm the idea of tectonic proximity of the root faults and shear zone. In the interaction area, minor fractures begin to develop and are progressively linked to the main faults. In the en échelon arrangement of the faults, the minor faults have grown and linked the en échelon segments of the faults. It seems that the earthquake ruptures can spontaneously propagate across both extensional and compressional fault steps. This propagation occurs along strike-slip faults such as Sabzevaran fault and its branches.

1. Introduction

Generally, faults progress as a network, within which the constituent faults can be presented by a range of lengths, sizes, and orientations. Different interactions can occur in a network as the fault form geometric and kinematic links with each other (e.g., Fossen et al., 2005; Frankowicz and McClay, 2010; Nixon et al., 2014; Duffy et al., 2015; Peacock et al., 2017). There has been noticeable interest in the interaction and linkage of stepping, sub-parallel, synchronously active faults, particularly dip-slip (e.g., Peacock and Sanderson, 1991; Leeder and Jackson, 1993; Walsh et al., 1999) and strike-slip ones (e.g., Wilcox et al., 1973; Rodgers, 1980; Woodcock et al., 1986; Dooley and Schreurs, 2012).

Some areas with local stress concentration and perturbation are produced by the fault interaction, which affects the geometry and kinematics of faults (e.g., Kattenhorn et al., 2000; Bourne and Willemse, 2001; Maerten et al., 2002; Rashidi et al., 2017, 2018). These stress concentrations can form the secondary structures in damage zones, where they typically have different orientations in comparison to the surrounding areas (e.g., Kim et al., 2004; Fossen et al., 2005; Bastesen and Rotevatn, 2012; Choi et al., 2016). It can cause a fault network, producing interactions between coeval faults, including connection of some faults (e.g., Peacock and Sanderson, 1991; Gawthorpe et al., 2003; Bull et al., 2006; Fossen and Rotevatn, 2016). Understanding the characteristics of these fault interactions is crucial as they can reveal convenient information about the tectonic deformation history.

The fault geometry, kinematics, and displacements are influenced by the way in which a fault interacts with other faults. Peacock et al. (2016, 2017) investigated the fault interactions represented in terms of: 1) The

* Corresponding author.
E-mail addresses: rashidi@iiees.ac.ir (A. Rashidi), abbassi@iiees.ac.ir (M.-R. Abbassi), faramarz.nilfouroushan@hig.se (F. Nilfouroushan), shafiei_shahram@uk.ac.ir (S. Shafiei), r.derakhshani@uu.nl (R. Derakhshani), majid_1974@uk.ac.ir (M. Nemati).

https://doi.org/10.1016/j.jsg.2020.104147
Received 19 December 2019; Received in revised form 19 July 2020; Accepted 20 July 2020
Available online 27 July 2020

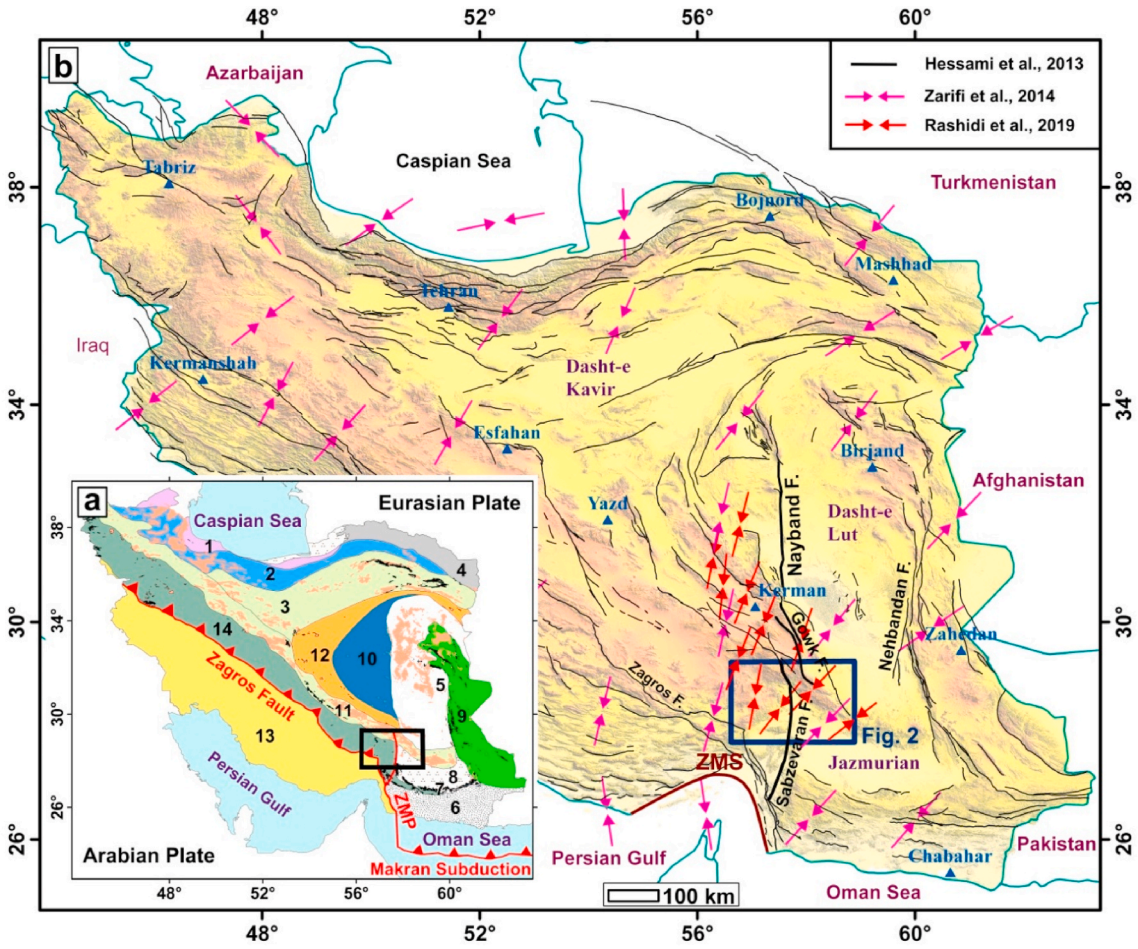

Fig. 1. (a) The structural zones of Iran. 1: Khazar-Talesh, 2: Alborz, 3: Central Iran, 4: Kopeh Dagh, 5: Lut Block, 6: Makran, 7: Ophiolitic Zone, 8: Jazmurian (Subzone of Makran), 9: Sistan, 10: Tabas (Subzone of Central Iran), 11: Urmieh-Dokhtar, 12: Yazd (Subzone of Central Iran), 13: Zagros, 14: SanandajSirjan and ZMP: Zendan-Minab-Palami Fault (b) Topographic map of the Iranian plateau with active faults (Hessami et al., 2013) and stress directions (pink arrows from Zarifi et al., 2014 & red arrows from Rashidi et al., 2019). The study area is marked by a blue box. ZMS is Zagros Makran Syntaxis. (For interpretation of the references to colour in this figure legend, the reader is referred to the Web version of this article.)

spatial arrangement of the faults, when fault planes have an intersection line, the interaction between them may or may not be geometrically linked (i.e. physically connected). 2) Kinematics of displacement distributions of the interacting faults and how the displacement directions are, i.e. parallel, perpendicular or oblique to the intersection line. 3) The status of the displacement in the interaction zones if the faults have similar or different displacement directions, and if the extension or contraction dominates in the acute bisector between the faults. 4) Chronology, i.e. the relative fault ages. This characterization scheme is used as a suggestion to classify interacting faults. Generally, Peacock et al. (2016) studied the kinematic, geometric and the topological relationships between faults and concentrated on how they relate to form networks. They also applied the term interaction to explain any relationship, where the development of one fault or other type of fracture affects others. We used their glossary of fault and other fracture networks in this paper.

In this paper, we focus on active faults in southeastern Iran (Fig. 1), where there are several N–S, NW-SE, NE-SW and E-W striking faults (Fig. 2). This area is a transitional zone between different structural zones i.e. Zagros, Sanandaj-Sirjan, Urmieh-Dokhtar, and Jazmurian (Back arc of the Makran subduction zone) (Fig. 1a). We present the important issue of the fault interactions between these structural zones. The addressed question is; how the active faults in the study area interact geometrically and kinematically, covering a range of structures in relay zones?

Previous active tectonic studies in this area only focused on Bam (e.g. Jackson et al., 2006; Fu et al., 2007), Gowk (e.g. Berberian et al., 2001; Meyer and Le Dortz, 2007; Walker and Jackson, 2002, 2004; Fattahi et al., 2014), Sabzevaran-Jiroft (Regard et al., 2005, 2009; Meyer and Le Dortz, 2007) faults (Fig. 2). However, so far, not so much investigation has been done on morphotectonics and the interaction between active faults in Sabzevaran area which are the focus in this paper.

Moreover, the study area and neighboring region were host of devastating and large intra-mountain and bordering fault earthquakes in modern history, e.g. the 1977 MS 7.0 Khurgu earthquake (Berberian and Papastamatiou, 1978), the 2003 MW 6.6 Bam earthquake (e.g.; Talebian et al., 2004; Fielding et al., 2005; Jackson et al., 2006), the 2006 MW 6.0 Tiab earthquake (Gholamzadeh et al., 2009) and the 2010–2011 MW 6.4–6.2 Rigan doublet earthquakes (Walker et al., 2013; Nemati, 2015). In the southwestern part of the study area, ~40 instrumental earthquakes with aftershocks ($5 \leq M \leq 6.6$; 1962–2020) occurred at different depths ($12\ km \leq d \leq 94\ km$), where there are interactions of NW-SE, N–S and NE-SW faults. It is also crucial to know the role of the active fault interaction and how they are related to the recent seismicity. To answer this question as well, we analyzed the geomorphological data related to each specific faults, field examples and earthquake catalogs.

2. Geology and tectonic setting

Complex tectonic evolution of Iran is related to the multistage

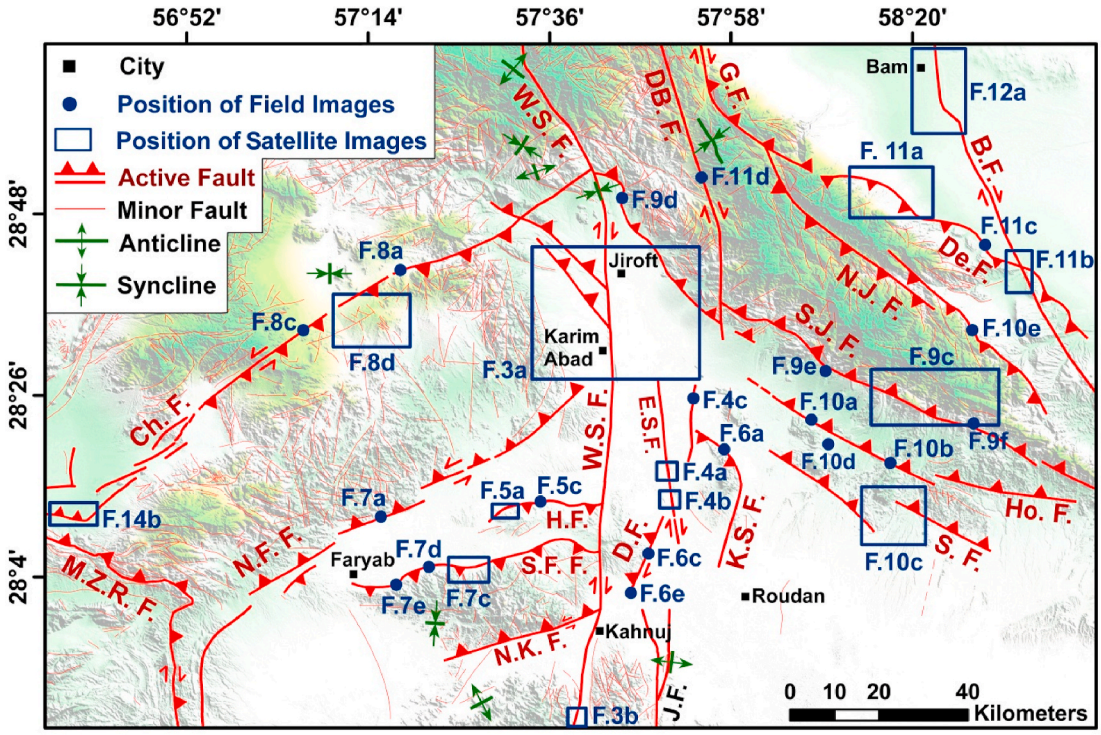

Fig. 2. Active faults of the study area on shaded relief map. B.F. = Bam Fault, De.F. = Dehno Fault, G.F. = Gowk Fault, N.J.F. = North Jebal-eBarez Fault, DB.F. = Dehbakri Fault, S.J.F. = South Jebal-e Barez Fault, Ho.F. = Hojatabad Fault, S.F. = Suru Fault, K.S.F. = Kuhe Suzgazi Fault, J.F. = Jiroft Fault, D.F. = Dehpish Fault, E.S.F. = East Sabzevaran Fault, W.S.F. West Sabzevaran Fault, Ch.F. = Chahmazrae Fault, N.F.F. = North Faryab Fault, H.F. = Heydarabad Fault, S.F.F. = South Faryab Fault, N.K.F. = North Kahnuj Fault, M.Z.R.F. = Main Zagros Reverse Fault.

history of the Tethys domain (Takin, 1972 and Stocklin, 1974). The accretion of the small continental blocks of Gondwanian affinity to Eurasia such as, Afghan, Lut, and Central Iran (sometimes is subdivided into Yazd and Tabas blocks) has resulted from the opening and closure of the large oceanic domains such as Neotethys (e.g. Berberian and Berberian, 1981; Meyer and Le Dortz, 2007). The subduction of the Neotethys beneath central Iran, sutured Iran and Arabian plates, and the subsequent continental convergence built the Zagros Orogenic Belt. This Orogenic belt (Fig. 1a) consists of three main NW-SE trending parallel zones: Urmieh-Dokhtar; Sanandaj-Sirjan and Zagros (e.g. Berberian et al., 1982; Agard et al., 2006, 2011; Shafiei et al., 2009, 2011, 2015). The study area consists of four structural zones: Urmieh-Dokhtar, Sanandaj-Sirjan, Zagros and Jazmurian (Back arc of Makran subduction) zones. The emplacement of the Urmieh-Dokhtar magmatic arc occurred during the Eocene and Oligocene. The Neotethys subduction has changed into a collisional stage at NW of the Hormoz strait, but continues actively to the south, offshore Makran (Agard et al., 2005). The northwest-striking Zagros fold and thrust belt is an active continental collision zone that corresponds to a continental accretionary prism within the Arabian Plate, accommodating about 10 $mmyr^{-1}$ of NNE-trending active shortening, between Arabia and Eurasia (e.g. Talebian and Jackson, 2002; Blanc et al., 2003; Hessami et al., 2006; Edey et al., 2020). To the east, the east-striking Makran belt is the emerged portion of an accretionary prism resulting from the still active subduction of the Oman oceanic lithosphere beneath the Iranian Plate (e.g. Byrne et al., 1992; McCall, 1997; Kopp et al., 2000; Nilforoushan et al., 2003; Burg, 2018). A NNW-striking deformation zone, the oblique reverse-dextral Zendan-Minab-Palami fault system (ZMP in Fig. 1a), connects the western Makran to the eastern Zagros deformation domains (Fig. 1) (McCall and Kidd, 1982; Regard et al., 2004; Derakhshani et al., 2005, 2011). The NNW-striking reverse-dextral ZMP fault system permits transfer of the deformation from the Zagros to the Makran prisms (e.g. Regard et al., 2004). The ZMP fault system is located at the plate boundary and its NNW trend is drastically oblique with respect to the direction of the convergence (e.g. Ross et al., 1986; Regard et al., 2004, 2009). It could have two major roles on a lithospheric scale: (1) to accommodate the plate convergence obliquity and (2) to transform the Zagros collision process into the Makran subduction (Meyer and LeDortz, 2007). Previous studies show that this transfer is accommodated by combined reverse and right-lateral faulting distributed over a wide domain (Regard et al., 2004; Rashidi et al., 2019).

The Sabzevaran fault system, as the longest fault in the our study area, is located at the ENE of ZMP fault, with a slip rate of ~5.7 ± 1.7 mm/yr (Regard et al., 2006) and is connected to the Nayband-Gowk fault system from the north side (Berberian, 1981; Walker and Jackson, 2002) (Fig. 1). It has a considerable contribution for transferring of the convergence deformation of the Iranian plateau northward to the tectonic settings such as the Alborz and Kopeh-Dagh mountain belts (e.g. Vernant et al., 2004 and Walker et al., 2009). Since a part of the deformation is accommodated by the numerous thrusts in the western and eastern compartments (Talebian et al., 2004 and Rashidi Boshrabadi et al., 2018, Savidge et al., 2019, Nemati et al., 2020), so the overall strike-slip motion accommodated by the Sabzevaran-Nayband-Gowk system is decreasing from the South to the North. In the south of study area, the Sabzevaran and Jiroft faults, are almost parallel (Fig. 2). These faults do not appear to be marked by any seismicity alignment even if the local seismicity level is high (Yamini-Fard, 2003). Sabzevaran-Jiroft faults are characterized by linear fault traces bounding the eastern flank of two ophiolite horsts, of Palaeozoic and Mesozoic ages (McCall et al., 1985). These East facing frontal fault zones consist of steep, fresh-looking scarps that mark the fault traces and are separated by undeformed zone that is about 15 km-wide (Meyer and Dortz, 2007; Regard et al., 2009). Both faults are segmented and affected the Quaternary alluvial fans and display evidence of geomorphic features. The linearity of both faults suggests that they are nearly vertical and accommodate dominantly strike-slip displacements (Regard et al., 2005).

The local and regional strain and stress fields in the Iranian plateau

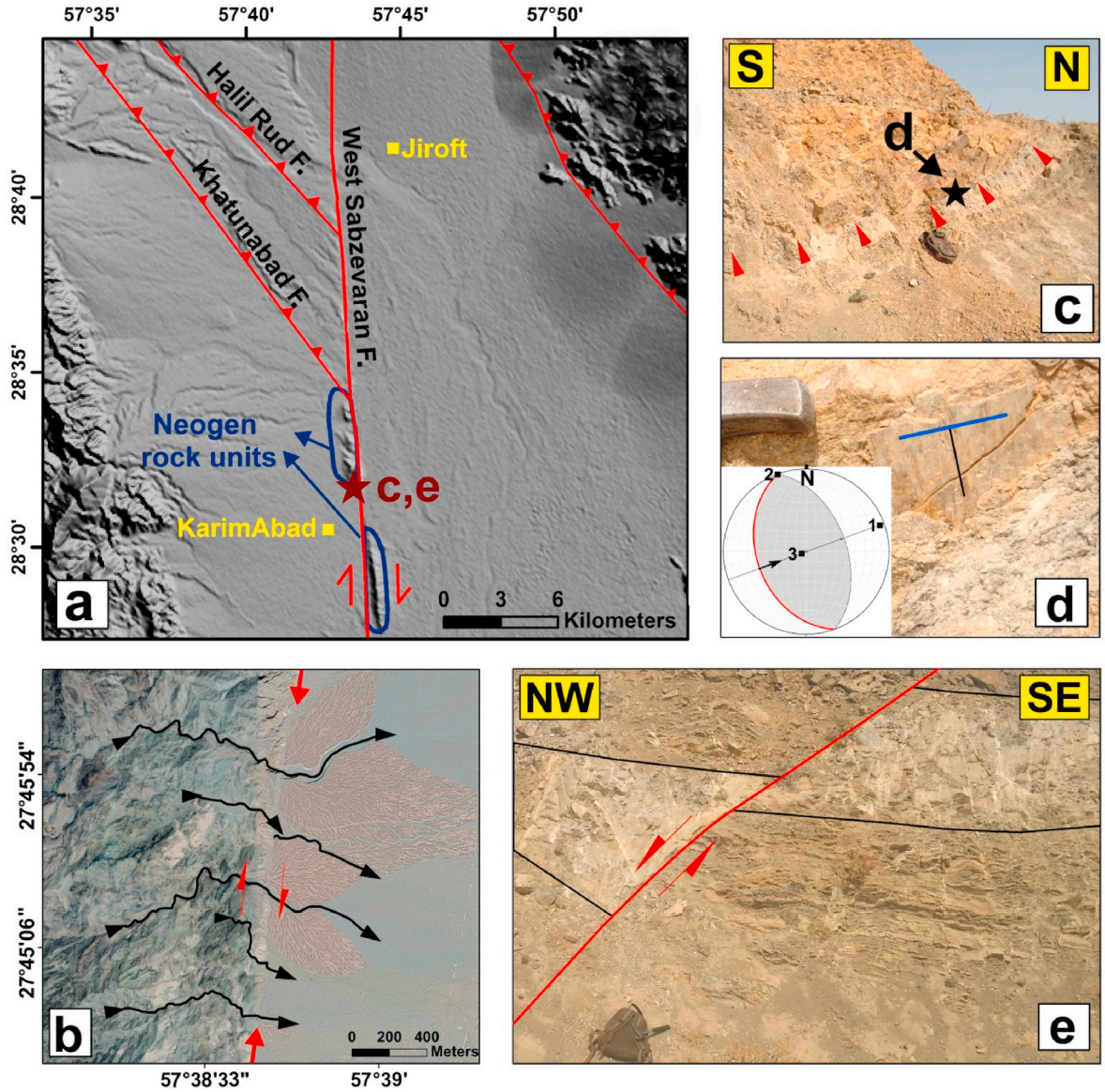

Fig. 3. (a) The 5.7 km right-lateral offset of Neogene rock units on the West Sabzevaran fault near Karim-Abad village. (b) ~200 m offsets and tilting of rivers along the fault. (c) Trace of a minor fault (340°, 40°SW) inside the West Sabzevaran shear zone with reverse mechanism (at 28°32′ N, 57°43′43″E). (d) Slickenline (250°, 90°) on the minor fault in part (c). Numbers 1, 2 and 3 in stereonet denote the orientations of the principal stress axes. Arrow in the stereonet indicates the movement direction of the hangingwall. (e) A minor fault inside West Sabzevaran shear zone with normal mechanism (at 28°30′11″N, 57°43′45″E).

were estimated and discussed in various studies (e.g. Masson et al., 2005; Peyret et al., 2009; Zarifi et al., 2014; Khodaverdian et al., 2015; Jentzer et al., 2017; Raeesi et al., 2017; Rashidi et al., 2019; Khorammi et al., 2019). The result of Focal Mechanism Stress Inversion (FMSI) analysis in the west and the south of the Lut block (Rashidi et al., 2019) shows a mean horizontal stress of N19°E under a transpressional tectonic regime. In the south and the west of the Lut block, the calculated rotation rates using the GPS velocities imply the maximum amount of clockwise rotation rate (~37 nanorad/yr) related to the Sabzevaran fault (Rashidi et al., 2019). Some small earthquakes have been recorded along the Sabzevaran fault (Fig. 13) and the absence of a main earthquake is noticeable.

3. Data and method

To characterize the type of active fault interactions, we used the offset and tilting of the rock units, especially in the Quaternary landforms. We investigated the geometry and kinematic of the faults by the slickenlines and the geomorphic phenomena along the faults. We used aerial photographs, digital elevation models, satellite images visualized in Google Earth and interpreted with the help of our morphotectonic field surveys. For those faults with kinematic indicator, we determined the principal stress directions using the kinematic "P" (shortening) and "T" (extension) axes method. These axes are equated with the principal stress directions σ1 and σ3, respectively. This method was reported as one of the most robust methods (Allmendinger et al., 1989).

Seismic activity data was used to deduce and interpret the morphotectonic data. The catalogue of instrumental earthquake in the period 1900–2006 from IIEES (International Institute of Earthquake Engineering and Seismology), ISC (International Seismological Centre), EHB (Engdahl Bulletin) and earthquake data between 2007 and 2019 from IRSC (Iranian Seismological Center) were used.

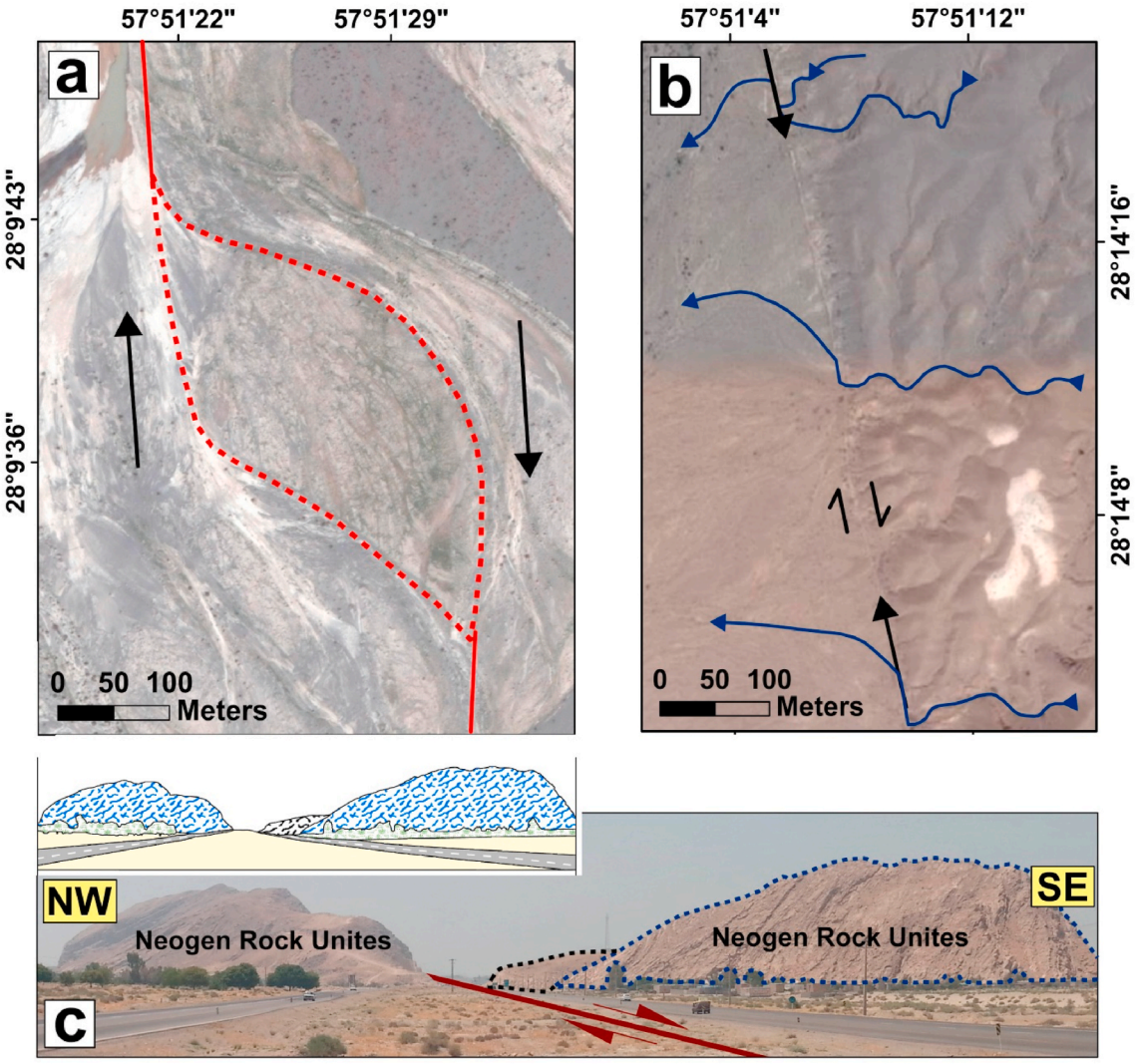

Fig. 4. (a) A pressure zone along the East Sabzevaran fault. (b) The ~100 m right-lateral offset of river by this fault. (c) The 110 m displacement of rock unites in Neogene along this fault (at 28°25′30″N, 57°49′15″E).

4. Structural evidence for active faulting

4.1. The Sabzevaran fault

The asymmetry between the eastern and western parts of the Zagros-Makran Syntaxis (ZMS in Fig. 1b) corresponds to shear zones proposed by Aubourg et al. (2004), in the hypothesis of the Oman peninsula acting as an indenter. The Sabzevaran fault is one of the main active faults in the transitional zone between Zagros, Makran and Central Iran (Regard et al., 2004) (Fig. 1b). This right-lateral transverse fault striking N–S shows evidence of Quaternary deformation. The Sabzevaran fault is accounted as a fault zone, which is divided into two parts namely the east and the west (Fig. 2).

4.1.1. The West Sabzevaran fault

The West Sabzevaran fault is about 300 km long, which in its southern part joins the ZMP fault (Fig. 1). This fault has cut and moved the Pliocene-Quaternary sediments. The cumulative offset along the fault is about 5.7 km in the Neogen deposits, which was estimated close to the Karim-Abad village (Fig. 3a). Moreover, there are ~200 m Quaternary offsets and deflection of rivers along the fault in alluvial fan (Fig. 3b). In the West Sabzevaran fault zone, a variety of minor branching faults with different mechanisms and orientations (reverse and normal with NW-SE and NE-SW strike, respectively) can be observed (Figs. 3c and e).

4.1.2. The East Sabzevaran fault

The East Sabzevaran fault with about 50 km long is located between Jiroft city, in southeast, and Kahnuj city, in northeast (Fig. 2). In some studies (e.g. Regard et al., 2005), the continuation of this fault in the east was introduced as Jiroft fault, which ends to 10 km away towards the east of Kahnuj city. The geometry of these faults are right step over types which causes a traction area (Fig. 2).

The Sabzevaran fault, especially in eastern part (in the Jiroft plain), is not traceable. The severe phase of water erosion and agricultural activities led to disappearance of this fault zone.

Along this fault, left bend contractional zones are observed, confirming the right-lateral movement of this fault zone (Fig. 4a). It also cuts and moves waterway and alluvial fans in its own way (Fig. 4b). According to morphotectonic and structural evidence, it is a right-lateral strike-slip fault with about 200 m displacement in the Neogene rock units (Fig. 4c).

4.2. The Heydarabad fault

The Heydarabad fault with reverse mechanism is about 30 km long

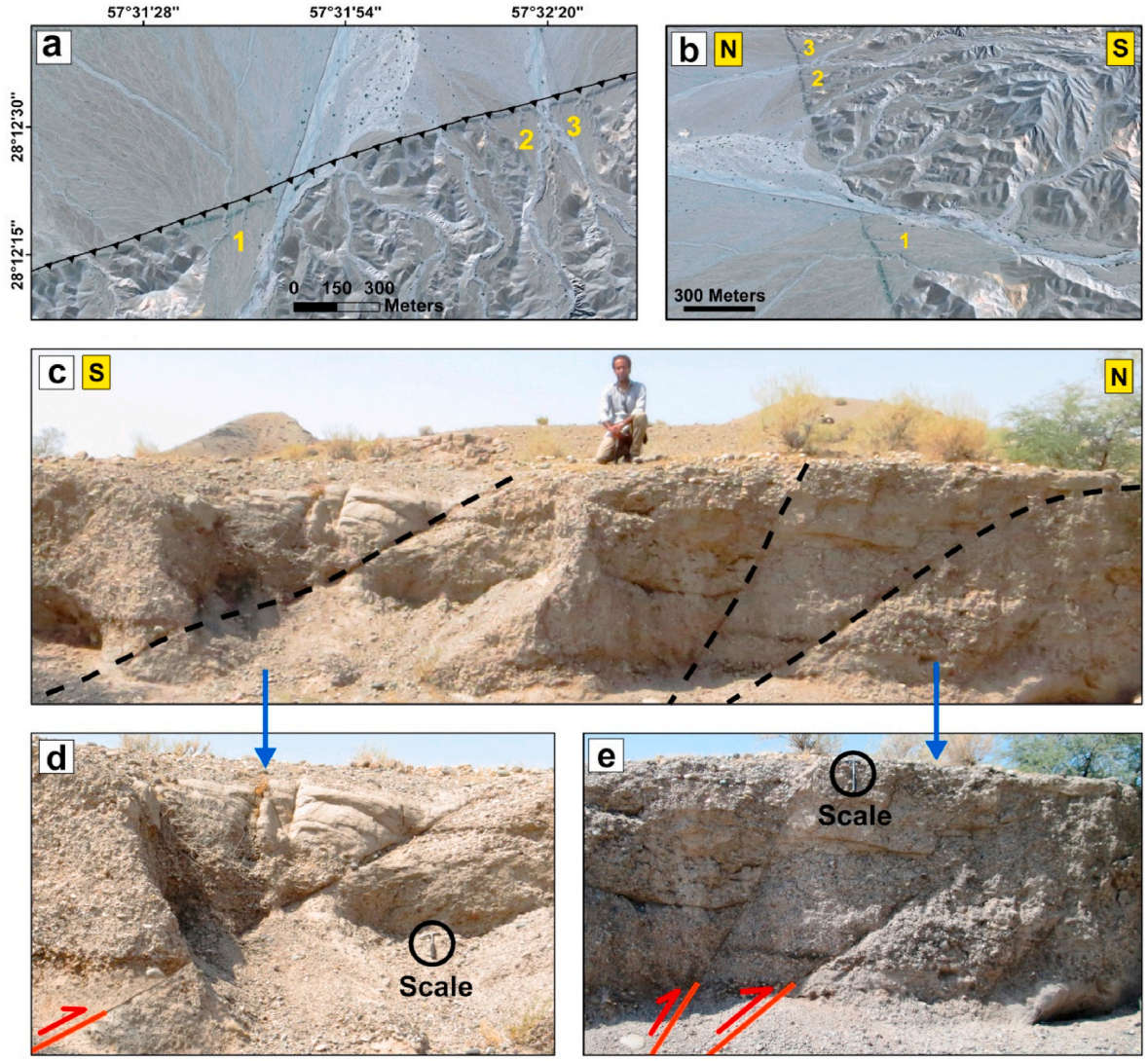

Fig. 5. (a) The trace of Heydarabad fault and uplifting in the alluvial fans 1, 2 and 3. (b) 3D image of uplifting in alluvial fans 1, 2 and 3 along Heydarabad fault. (c) Field photo of the Heydarabad fault zone (at 28°12′41″N, 57°35′ E). (d) and (e) illustrate faulting in closer view.

located in the south of Heydarabad village (Fig. 2) lies almost perpendicular to the West Sabzevaran fault. The surface expression of the Heydarabad fault is linear with a gentle curvature in the mountain front zone and the plain. Uplifted alluvial fans along this fault are the most significant markers which show the active uplift along the fault zone (Fig. 5a and b). Our observations during the field work also indicated the Heydarabad fault crosscuts clearly the alluvial fans and their Pliocene-Quaternary deposits (Fig. 5c).

4.3. The Kuhe Suzgazi fault

In the east of Sabzevaran fault zone, the Kuhe Suzgazi fault with curved geometry runs in a mountain ridge with the same name. The southern segment with NE-SW strike is a right-lateral transpressional fault. However, the northern segment with attitude 140°, 45°SW, and its slickenline with striation 200°, 40° act as reverse segment (Fig. 6a and b).

4.4. The Dehpish fault

The Dehpish fault with about 25 km long and a right-lateral strike-slip component is located between the West and the East Sabzevaran faults (Fig. 2). The cutting and uplifting rock units, and the displaced waterways are the morphotectonic evidences which we could find along the fault (Fig. 6 c, d, e).

4.5. The North Faryab fault

The North Faryab fault with attitude 55°, 60° NW and 90 km long is located in the north of Faryab city (Fig. 2). This fault consists of three main segments arranged in left-step manner, with documented seismic activity (Fig. 13).

The North Faryab fault potentially can be accounted as a source of seismic hazards for the Faryab city and surrounding area. The morphotectonic evidence along this fault, such as displacement in the rock units and rivers, confirm its activity in different time. Migration of the fault scarp on the footwall is one of the significant structural phenomena (Fig. 7a). In each phase of activity, the exposed area is characterized by the scarps parallel to the fault strike. The rock units are folded along the scarps showing the fold related faulting (Fig. 7b).

4.6. The South Faryab fault

The South Faryab fault with attitude 080°, 65° S and its slickenline with striation 195°, 65° is known as a reverse fault (Fig. 7e and f). The length of the fault is about 70 km (Fig. 2). The geometry of the alluvial

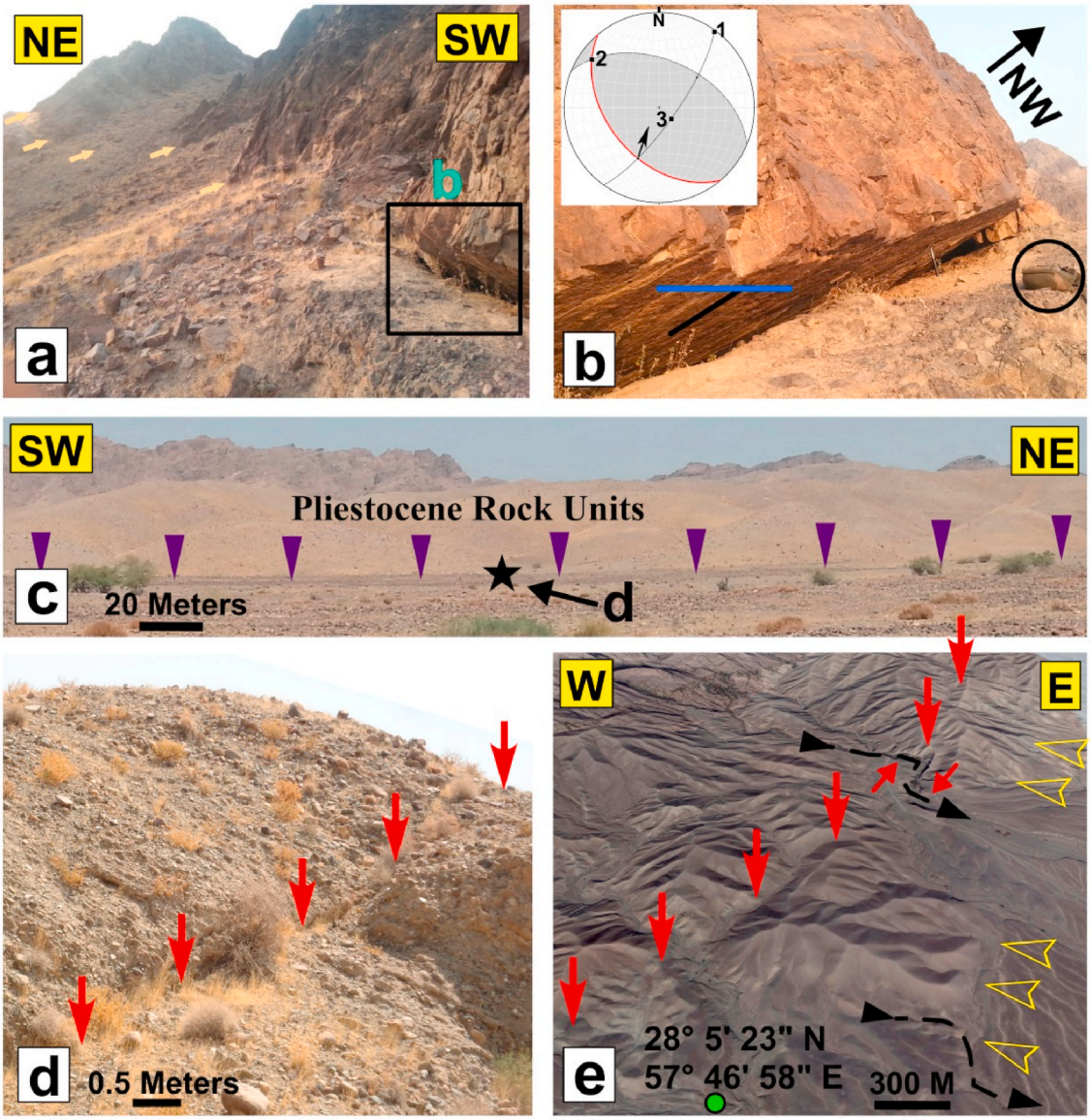

Fig. 6. (a) Field photo of the northern segment of Kuhe Suzgazi fault with attitude 140°, 45°SW (at 28°18′15″N, 57°57′13″E). (b) The fault trace from a closer view with slickenline on its plane (200°, 40°). Numbers 1, 2 and 3 in stereonet denote the orientations of the principal stress axes. Arrow in the stereonet indicates the movement direction of the hangingwall. (c) Uplifting of Pliestocene rock units along the Dehpish fault (at 28°6′3″N, 57°47′30″E). (d) Faulting in a alluvial fan along the fault. (e) Right lateral offsets of the rivers by the Dehpish fault.

fans in the western and central parts of this fault is used as indicator to deduce its reverse faulting mechanism (Fig. 7c). In the alluvial fans, fault scarps can be observed related to the south Faryab fault (Fig. 7d). The noticeable high uplifted alluvial fans along the south Faryab fault scarps indicate the high activity of this fault.

4.7. The Chahmazrae (Esfandaqe) fault

The Chahmazrae fault with about 25 km long, and attitude 045, 60 SE is parallel to the North Faryab fault (Fig. 2). The rock units have over thrusted along it (Fig. 8a). The slickenline measurements on the fault plane (striation: 200°, 35°) indicates a left-lateral strike-slip mechanism with a reverse component (Fig. 8b). The activity of Chahmazrae fault and its back thrust (Fig. 8c) led to Pop-Up structures.

The high activity of the Chahmazrae fault formed considerable shear zones on the hanging wall, manifested by shear zones faults, as R and R' (Fig. 8 d, e). In Fig. (8 f, g) a R shear is dextrally offset by a R′ shear for about 500 m and a R′ shear is sinistrally offset by a R shear for about 300 m.

4.8. Faults in the Jebal-e Barez Mountain range

In the Jebal-e Barez Mountains (Figs. 2 and 9a), several NW-striking faults cut through geological units (Babakhani and Alavi Tehrani, 1992). Morphotectonic evidence (such as the folding and uplifting in the Quaternary units, displacement and deflection of waterways and rock units) indicates high activity related to these fault systems. According to the geometry and mechanisms of the faults in the Jebal-e Barez Mountain range, the positive flower structure is suggested for this part of our study area (Fig. 9b).

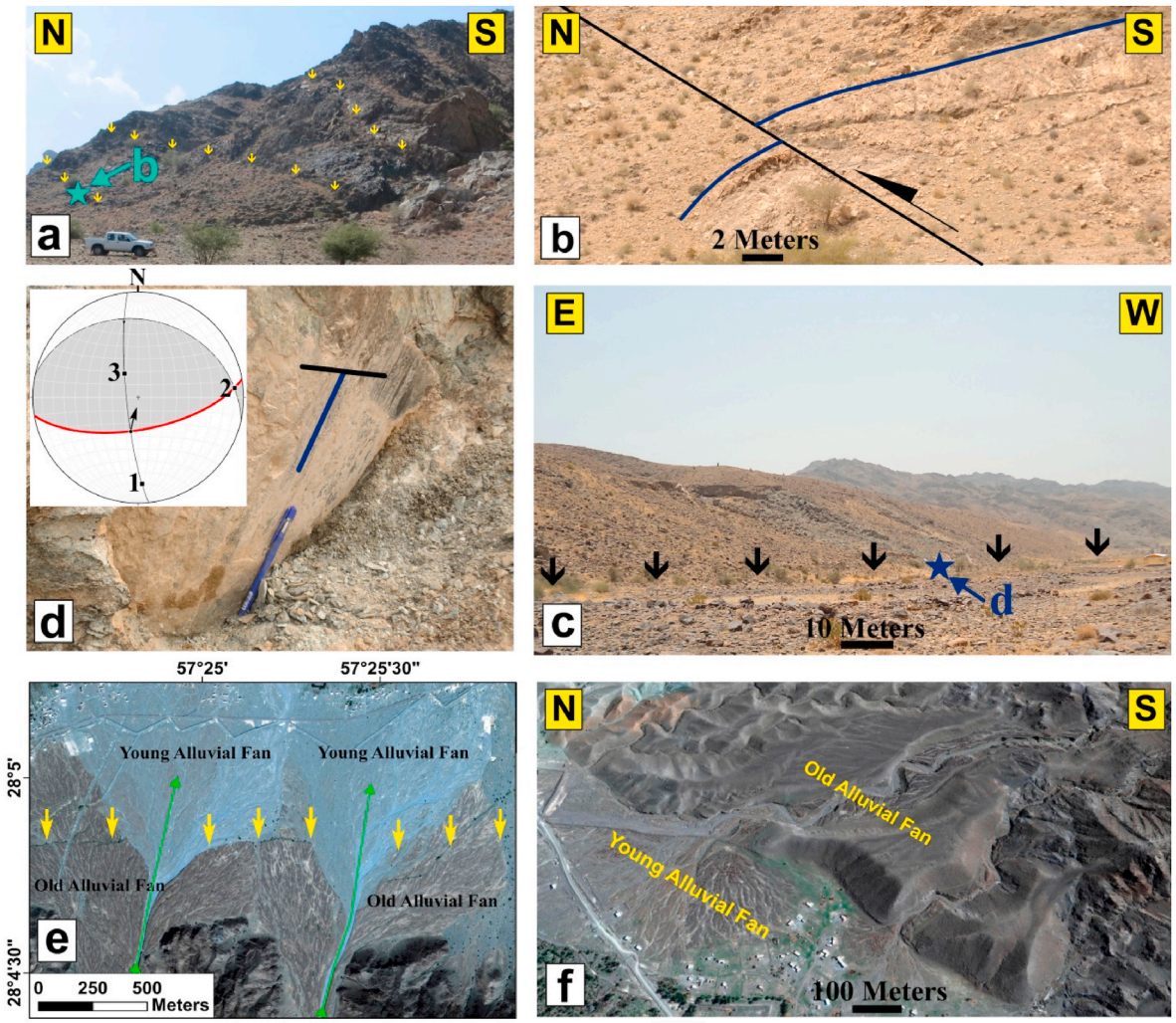

Fig. 7. (a) The North Faryab fault zone. The fault scarp migration is one of the significant structural phenomena (at 28°12′23″N, 57°19′17″E). (b) Folding related to the North Faryab fault. (c) Trace of South Faryab fault (black arrows) with attitude 80°, 65° SE (at 28° 2′18″N, 57°15′60″E). (d) The fault trace from a closer view with slickenline on its plane (193°, 65°). Numbers 1, 2 and 3 in stereonet denote the orientations of the principal stress axes. Arrow in the stereonet indicates the movement direction of the hangingwall. (e) Trace of South Faryab fault (yellow arrows) inside alluvial fans. Growth of the young alluvial fans, in central part of the old alluvial fans, is because of reverse mechanism of South Faryab fault. (f) The 3D images of uplifting the old alluvial fans along the south Faryab fault (at 28° 4′24″N, 57°20′5″E). (For interpretation of the references to colour in this figure legend, the reader is referred to the Web version of this article.)

4.8.1. *The South Jebal-e-Barez fault*

The south Jebal-e Barez fault runs for about 200 km (Fig. 9a), and reveals a sharp linear trace (Fig. 9c). We found the youngest plains of the fault among the Eocene and Quaternary rock units (Fig. 9d). There are imbricate structures that those consists of a series of overlapping rock slices separated by sub-parallel reverse faults (Fig. 9e and f). The South Jebal-e-Barez fault consists of three main segments with left-step geometry (Fig. 2). Fault segments mechanism are reverse with a little left-lateral strike-slip component. So, middle segment with attitude 310, 70 NE has slickenline with striation 065°, 70° (Fig. 9f).

4.8.2. *The Hojatabad fault*

The Hojatabad fault with about 75 km long and attitude 310, 50 NE lies in the south of the Jebal-e Barez fault, including two segments with left-step pattern (Fig. 2). In response to its activity, Quaternary units are folded and formed tear faults (Fig. 10a and b). The uplifted alluvial fans along the fault indicate the high activity of this fault.

4.8.3. *The Suru fault*

The Suru fault with about 50 km long is located in the south of Hojatabad fault (Fig. 2). This fault consists of two left-stepped segments, in which there are some folds in the crossing location (Fig. 10c). The rotation of rock units along this fault has caused changing in the alluvial fans. Recumbent folds in the area between the Suru and the Hojatabad faults were formed, because of pressure and reverse component of these faults (Fig. 10d).

4.8.4. *The North Jebal-e Barez fault*

The north Jebal-e Barez fault with 90 km long and attitude 315, 30 SW is included two left-stepped segments (Fig. 2). The Slickenline of the fault with striations of 55°/70° show reverse mechanism (Fig. 10f). The fault has cut rock units especially recent sediments along itself (Fig. 10e).

4.8.5. *The Dehno fault*

The hidden Dehno fault with about 70 km long has a curved geometry (Fig. 2). In response to its activity, Quaternary units are uplifted (Fig. 11a and c). The trace of the Dehno and Bam faults, on the satellite images, indicate these faults interacted with each other in the northeast of Ghale- Dokhtar village (Fig. 11b).

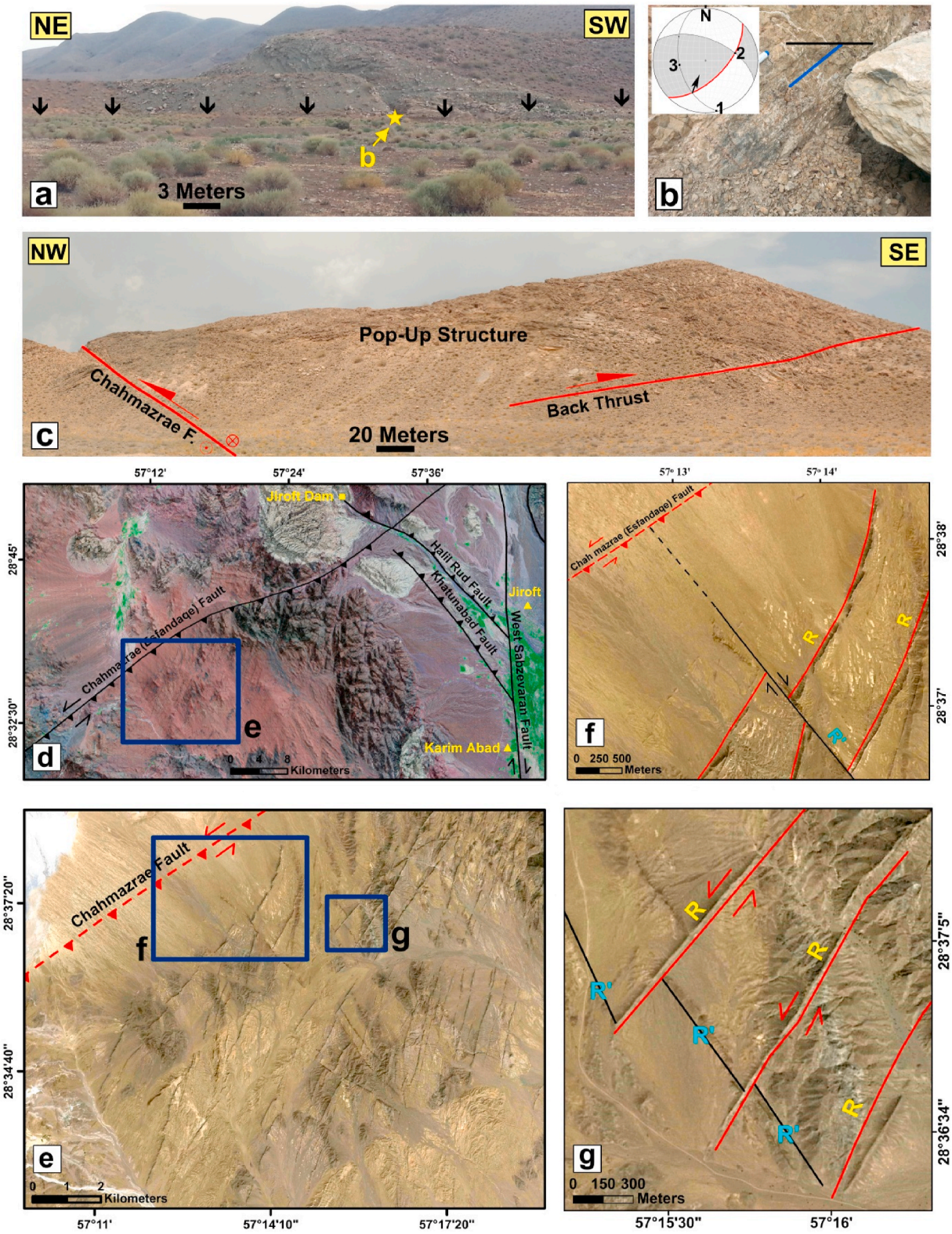

Fig. 8. (a) The trace of Chahmazrae fault and uplifting in the young rock units with attitude 45°, 60° SE (at 28°40′30″N, 57°17′22″E). (b) Slickenline of the fault with striations of 200°/35°. Numbers 1, 2 and 3 in stereonet denote the orientations of the principal stress axes. Arrow in the stereonet indicates the movement direction of the hangingwall. (c) The Pop-Up structure related to the activity Chahmazrae fault and its back thrust (at 28°30′54″N, 57° 1′58″E). (d) The Chahmazrae fault with its surrounding main faulting. The location of shear zones related to the Chahmazrae fault has been shown by a blue box. (e) The shear zones on the hanging wall of Chahmazrae fault. (f) and (g) The growth of R and R′ faults correspond to the activity of Chahmazrae fault. (For interpretation of the references to colour in this figure legend, the reader is referred to the Web version of this article.)

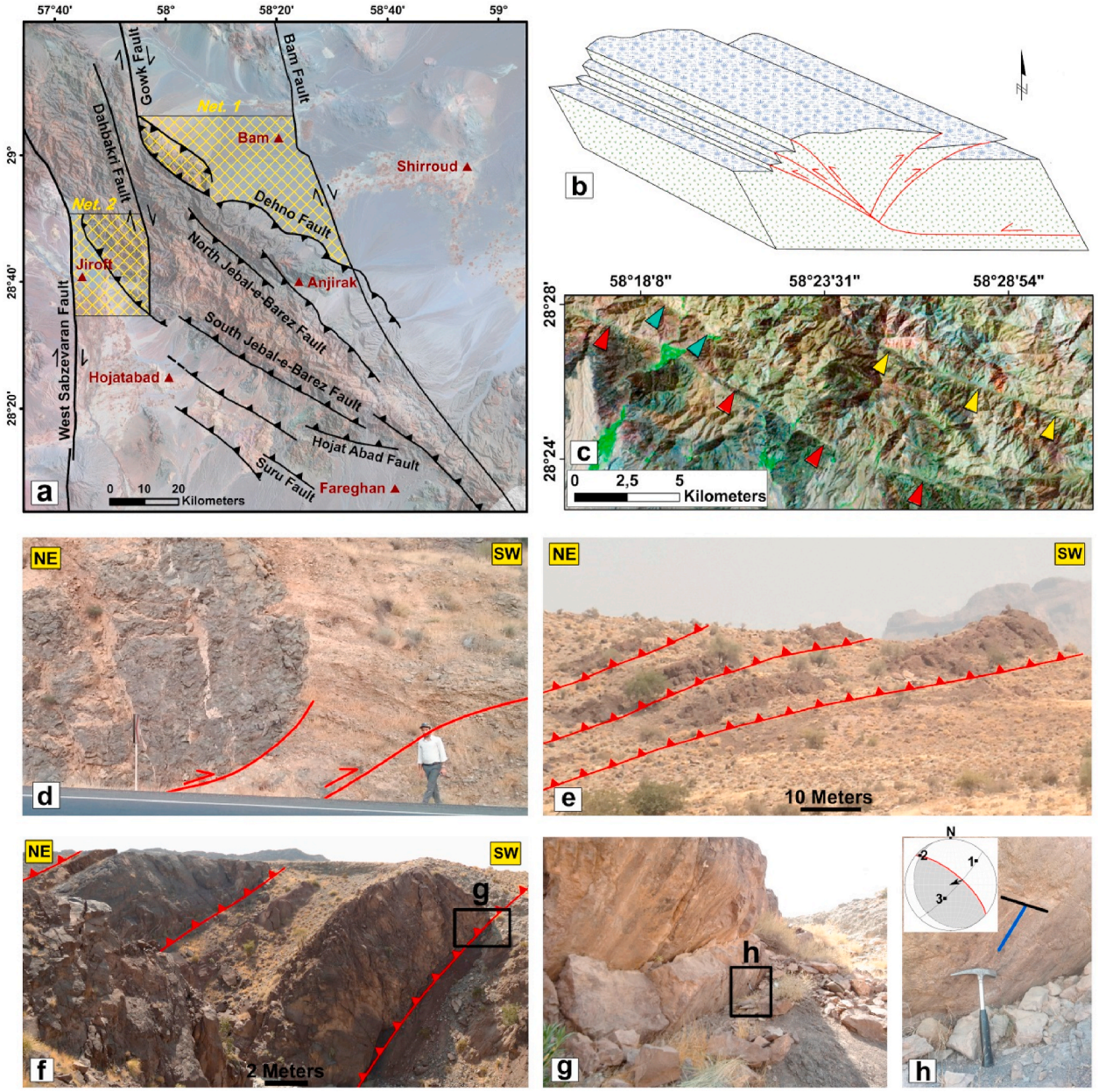

Fig. 9. a) The main active faults in the Jebal-e Barez area. b) The positive flower structure is the suggested schematic tectonic model for this area. (c) Sharp trace of the South Jebal-e Barez fault Zone. (d) Emplacement of Eocene Pyroclastics on the Quaternary units by reverse faulting in the South Jebal- e Barez fault zone (at 28°46′55″N, 57°46′ E). (e), (f) Repetition of Eocene rock units by South Jebal-e Barez fault zone (at 28°28′52″N, 58°10′14″E and 28°22′48″N, 58°23′26″E). (g) The trace of a branch of the South Jebal-e-barez fault in closer view with attitude 310°, 70° NE (h) Slickenline of the fault with striations of 070°/70°. Numbers 1, 2 and 3 in stereonet denote the orientations of the principal stress axes. Arrow in the stereonet indicates the movement direction of the hangingwall.

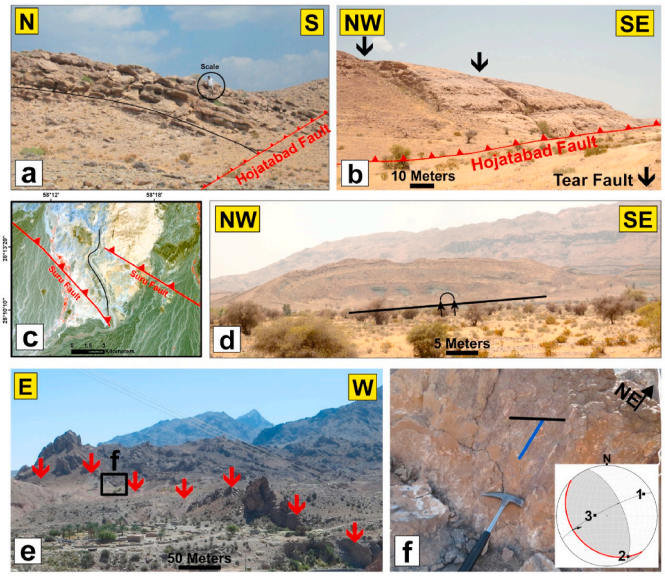

Fig. 10. (a) The folding of the Quaternary rock unit along the Hojatabad fault (at 28°21′41″N, 58°09′51″E). (b) Tear faults on the Hanging wall of Hojatabad fault (at 28°18′40″N, 58°15′50″E). (c) The rock unit folding between the segments of Suru fault. (d) Recumbent fold in the area between Suru and Hojatabad faults (at 28°20′29″N, 58°10′8″E). (e) The trace of the North Jebal-e Barez fault with attitude 135°, 30° SW (at 28°33′50″ N, 58°27′40″ E). (f) Slickenline of the fault with striations of 250°/30°. Numbers 1, 2 and 3 in stereonet denote the orientations of the principal stress axes. Arrow in the stereonet indicates the movement direction of the hangingwall.

4.8.6. *The Dehbakri fault*

We believe the continuation of the Gowk fault is the Dehbakri fault (Fig. 2). This fault with about 80 km long has NNW strike and an ENE-ward dip (Fig. 11d). There are some nearby earthquakes which could be related to the Dehbakri fault. Most of the significant earthquakes could be assigned to this fault e.g. the October 06, 2004 earthquake with magnitude 5.2 (no. 3 in Fig. 13). According to the focal mechanism solution of this earthquake (from Harvard CMT), the fault has a right-lateral strike-slip component. Some folds in the Dehbakri fault can be observed (Fig. 11d).

4.9. *The Bam fault*

The N–S striking Bam fault with length of about 100 km passes near the Bam city (Aghanabati et al., 1993) (Figs. 2 and 12a). The young fault scarp and displacement of the alluvial fans in the Bam plain indicate the fault activity in the Quaternary. After the Bam earthquake in 2003 (Mw~6.6), the length of the fault was revised and extended to more than 100 km (e.g. Talebian et al., 2004; Fielding et al., 2005; Jackson et al., 2006) (Fig. 12). According to the field observations and the mechanism of the main shock, mechanism of the fault is right-lateral strike-slip (Figs. 11b and 12).

In general, our study area is characterized by active fault systems with different strikes and faulting mechanisms. Their geometry and kinematics were worked out by the field studies and morphotectonic analysis (summarized in Table 1).

5. Interacting faults in the study area

To characterize the type of fault interaction, we need to know the fault surface traces and their geometric-kinematic characteristics (section 4). The description of the range of different fault interactions in this section was an attempt to determine fault interactions, applicable to all fault classes (normal, reverse, strike-slip and oblique-slip) at all scales and tectonic setting (Peacock et al., 2016, 2017). In this section, we used Peacock et al. (2017; Fig. 15), for describing fault patterns, especially in understanding related deformation patterns. We characterized the geometric-kinematic relationships, angles between the intersection lines (the line along which faults meet) and displacement directions, the strain that occurs at and around the interaction or intersection zones, and on the relative age relationships of the interacting faults. Using these parameters, we have presented some relationships/a relationship between the faults and structural zones (Tables 2 and 3). In two dimensions some faults have no interaction with other faults (e.g. Hojatabad and Suru faults). Some faults exposed in the study area are characterized by their segmentation. For example, the N–S fault zones Bam, Gowk, Sabzevaran, Jiroft are composed of a series of interacting and linked segments.

In the study area the most tectonic deformation are concentrated in the special structural zones such as: strike-slip zones and transpressional zone in particular, North Faryab-Chahmazrae. This concentrated deformation can be in a range of forms, including minor faults such as Heydarabad fault. In the southwestern of the study area, we suggested a triple relationship of fault interaction between the MZRF, NFF and ZMPF where many earthquakes occurred (Table 2, and Figs. 14 and 15).

The faults reviewed in this article have caused a number of the earthquakes within specific structural zones and at the interaction of faults (Fig. 13). About 40 instrumental earthquakes and aftershocks ($5 \leq M \leq 7$; 1962–2020) with focal depth between 12 km and 94 km occurred in the SW of study area (Fig. 14).

6. Seismicity

In the study area, the seismogenic zone has an average of 18 km depth, while Moho discontinuity is at ~49 km depth (Gholamzadeh et al., 2014). Seismogenic depth was determined, based on local seismological data of aftershock surveying of the 1990 Darab earthquake (Walker et al., 2005), the 2003 Bam earthquake (Tatar et al., 2005), the 2006 Tiab earthquake (Gholamzadeh et al., 2009) and the 2010–2011 Rigan earthquakes (Walker et al., 2013) at the west, northeast, southwest and southeast of the study area, respectively.

In the study area, two distinct earthquakes occurred: firstly the shallow one (blue symbols with less than 18 km depth in Fig. 13) and secondly the ones with intermediate depth (green symbols, with more than 18 km depth in Fig. 13).

Generally, based on the earthquake distribution (Fig. 13), clusters with a large extent could be recognized. Some of the events in these clusters are related to the Kahnuj, South Faryab, Heydarabad, Suru, Dehbakri, Bam faults, and Chahmazrae-North Faryab shear zone. This Shear zone is 30 km width and 100 km length and appear as a series of elongated depressions bounded by sets of oblique faults (North Faryab and Chahmazra faults). This shear zone is expressed as a transpressional zone with a set of Riedel and normal faults (Fig. 15). Stress accumulation on the faults and shear zone may be responsible for shallow and deep seismicity. The number of events increases toward the southwest mostly inside Chahmazrae-North Faryab shear zone, which is a severe seismic hazard for neighboring cities. The fault activity of the Chahmazrae, the North Faryab and their Riedel shear structures could be due to vicinity to the Main Zagros Reverse fault (MZRF) (Fig. 2), accommodating about 10 mm/yr of shortening (Regard et al., 2005).

The 28 February 2006 Tiab earthquake (M_W 6.0), is one of the largest instrumental earthquakes in the SW study area (Table 4) (marked by No. 16 in Fig. 13). Locally, well-located aftershocks of this event were distributed at 11–22 km depth. The focal mechanism of the main shock indicates a thrust mechanism, while most of the focal mechanisms of the aftershocks are dominantly strike-slip, indicating slip partitioning in depth (Gholamzadeh et al., 2009). The depths of the aftershocks in this region are well determined by the occurrence of microseismicity in shallow crust (Gholamzadeh et al., 2009); rather these are almost the same as focal depths of recorded microseimicity in the transition zone located in the east of the Zendan– Minab– Palami (ZMP) fault system

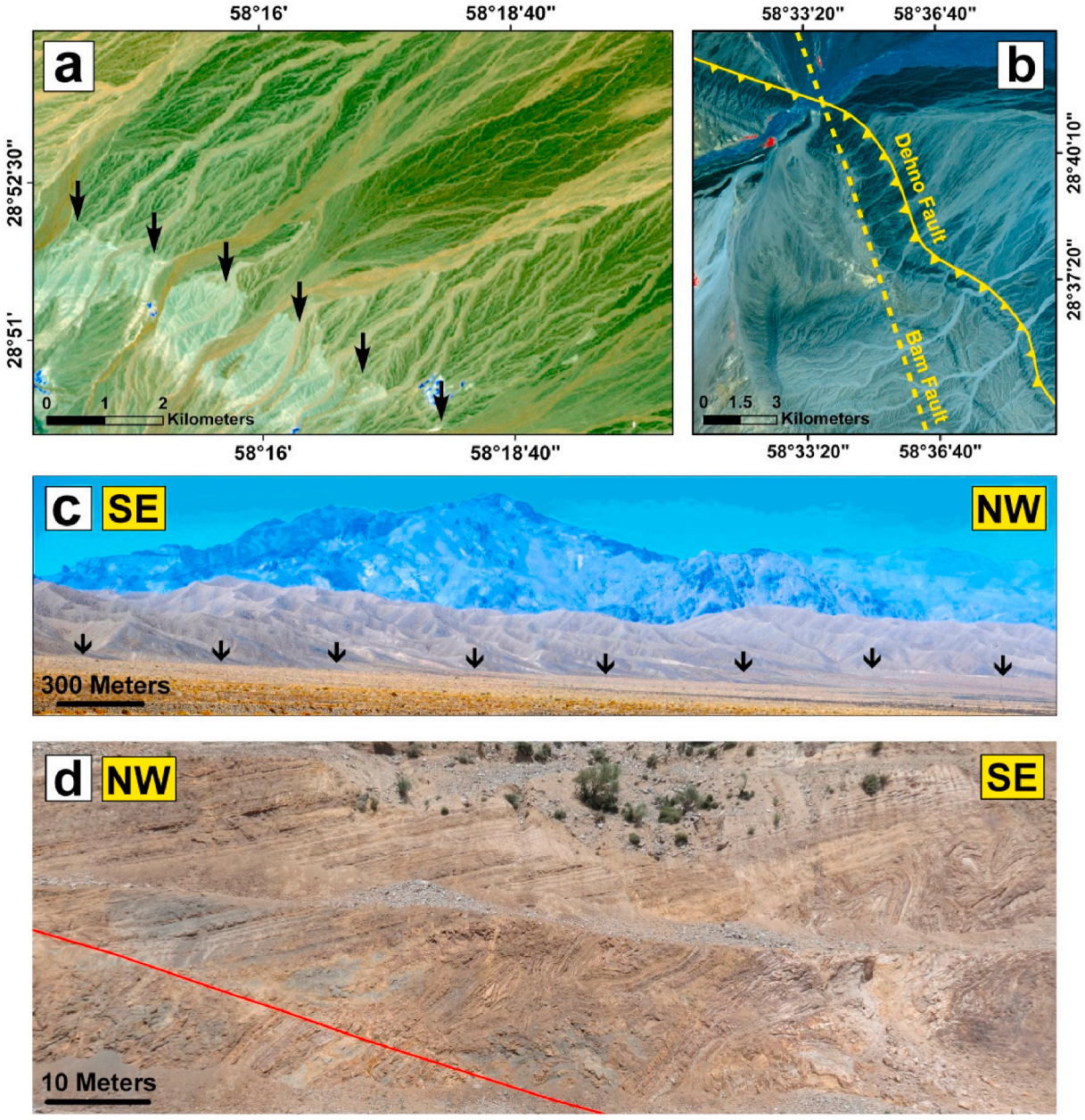

Fig. 11. (a) Trace of Dehno fault and uplifting the alluvial fans along the fault. (b) The crossing location of the Dehno and Bam faults. (c) A field photo illustrating the uplift in Quaternary sediments by the Dehno fault (at 28°43′25″ N, 58°29′5″ E). (d) The Dehbakri fault and folding of the rock units along that fault (at 28°56′30″N, 57°53′30″E).

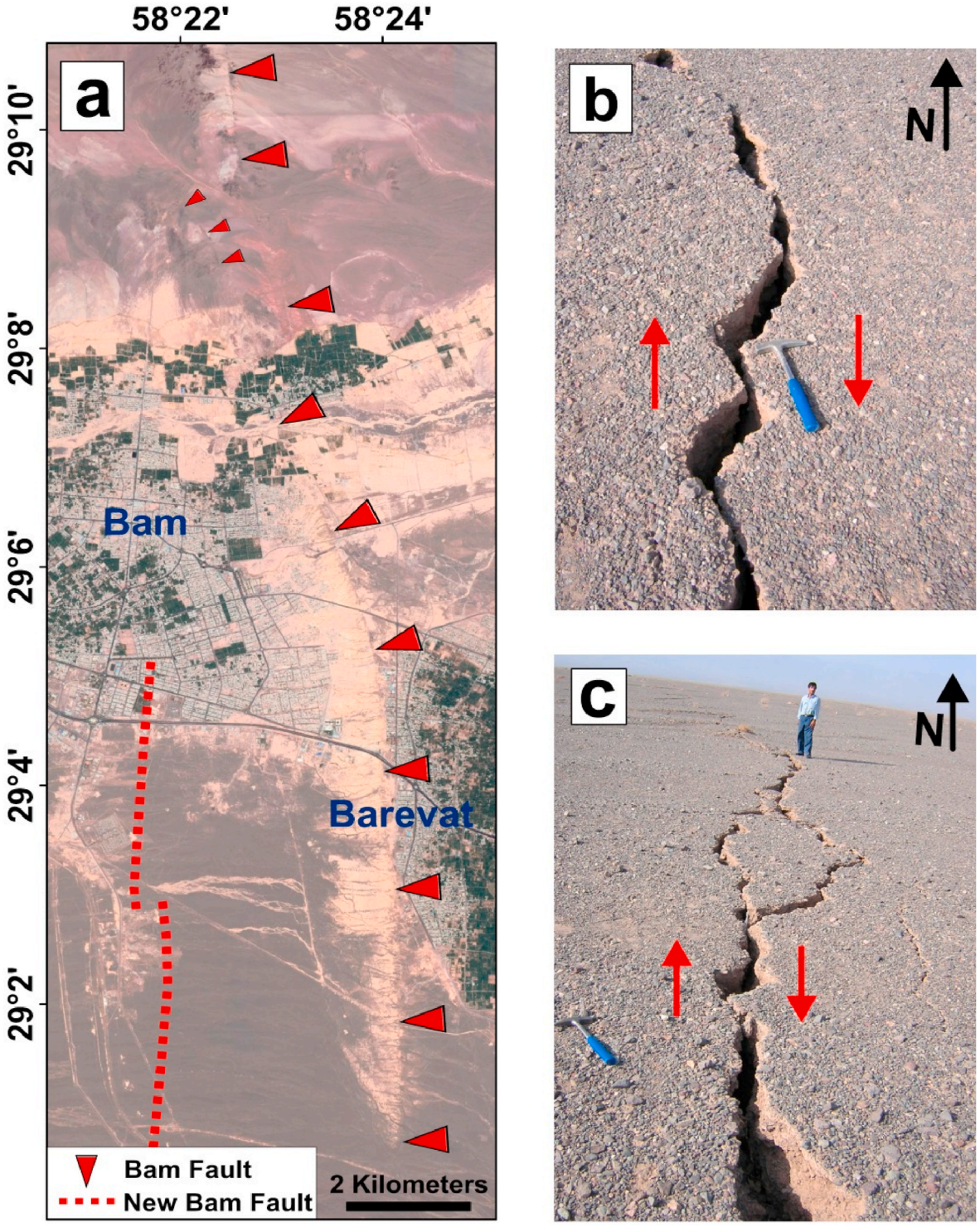

Fig. 12. (a) The attitude of Bam fault in around Bam and Baravat city. (b) and (c) The rupture of the fault in the 2003 Bam earthquake shows right lateral offset (at 28°40′11″ N, 58°21′35″ E).

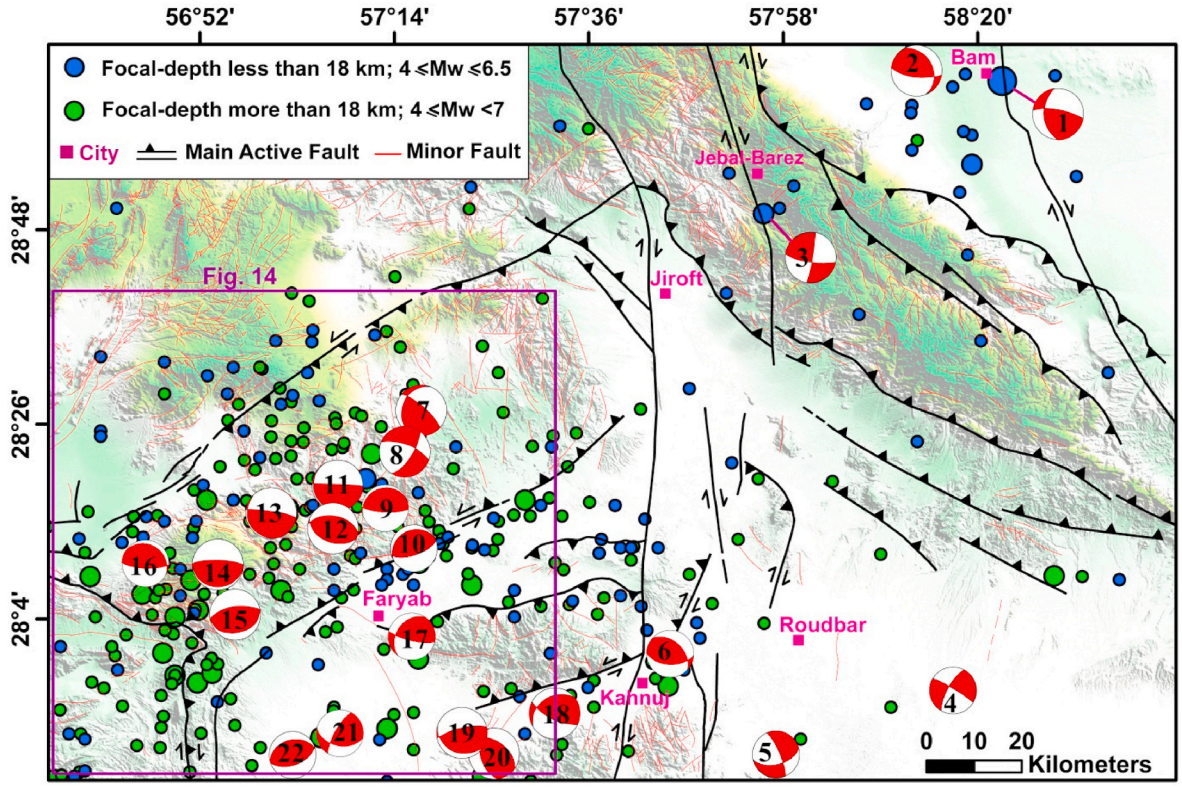

Fig. 13. Instrumental earthquakes with different depth in the study area. The specifications of focal mechanism solutions are given in Table 4.

Table 1
Specifications of the faults and their mechanism in the study area. See location of the faults in Fig. 2.

Name fault	Number of the main Segments	Approximate total fault length (Km)	Attitude (or strike) of the fault	Fault Mechanism (on the basis of; slickenlines and geomorphology data)	Related Figures
West Sabzevaran	3	300	NS	Right Lateral Strike Slip	Fig. 3
East Sabzevaran	1	50	NS	Right Lateral Strike Slip	Fig. 4
Heydarabad	1	30	EW	Reverse	Fig. 5
Kuhe Suzgazi	1	35	N40W, 45SW	Reverse and Right Lateral Strike Slip	Fig. 6a and b
Dehpish	1	25	NE-SW	Right Lateral Strike Slip	Fig. 6c,d,e
North Faryab	3	90	N55E, 60NW	left-lateral strike-slip with a reverse	Fig. 7a and b
South Faryab	1	70	N80E,65SE	Reverse	Fig. 7c–f
Chahmazrae (Esfandaqe)	3	120	N50E, 65SE	left-lateral strike-slip with a reverse	Fig. 8
South Jebal-e-Barez	3	200	N30W, 70NE	Reverse with a little Left Lateral Strike-Slip	Fig. 9c–h
Hojatabad	2	75	NW-SE	Reverse	Fig. 10a and b
Suru	2	50	NW-SE	Reverse	Fig. 10c and d
North Jebal-e Barez	2	90	N45W, 30SW	Reverse	Fig. 10e and f
Dehno	1	70	NW-SE	Reverse	Fig. 11
Dehbakri	1	80	NS to NW-SE	Right Lateral Strike Slip	Fig. 12
Bam	2	100	NS to NW-SE	Right Lateral Strike Slip	Fig. 13

(Yamini Fard et al., 2007). These earthquakes Table 5 could confirm the idea of tectonic proximity of the root faults and shear zones.

The earthquakes associated with focal mechanism (Fig. 13) could be assumed within a few different categories, based on their mechanisms and depths. It is significant that most of the earthquakes #7–16, occurred within the Chahmazrae-North Faryab shear zone, are reverse and belong to deeper crust (>18 km). According to their depths, their distances to the MZRF and MZRF dipping in this area (~50°; Regard et al., 2009), this fault could be the source of these earthquakes.

In addition, there are no significant earthquakes in the Instrumental Earthquake Catalogue in the northwestern part of the study area. The lack of seismicity in this part is questionable and is important because seismic faults which affect Quaternary sediments can also be traced on the satellite images.

7. Discussion

Geometric-kinematic characteristics of the faults, presented in section 4, are affected by interaction of fault zones. As mentioned before, fault interactions are represented in terms of: the spatial arrangement of the faults, kinematics of displacement distributions of the interacting faults, the status of the displacement in the interaction zones, and the chronology (Peacock et al., 2016). Peacock et al. (2016) presented a rational and consistent set of terms to explain how two or more faults interact kinematically and geometrically, covering some structures from relays, through closing and adjacenting fractures, to cross-cutting

Table 2
Type of interactions that the faults created with each other in the study area.

Relationship of the faults	Faults
Approaching	North Faryab_ West Sabzevaran
	South Faryab_ North Faryab
	West Sabzevaran_ Dehpish
	East Sabzevaran_ Dehpish
	East Sabzevaran_ Hojat Abad
	Suru_ Kuhe Suzgazi
	Hojatabad_ Bam
	Hojatabad_ Dehbakri
	Hojatabad_ South Jebal-e Barez
	South Jebal-e Barez_ Bam
	North Jebal-e Barez_ Bam
	South Jebal-e Barez_ North Jebal-e Barez
Abutting	West Sabzevaran_ South Jebal-e Barez
	West Sabzevaran_ Chahmazrae
	West Sabzevaran_ Heydarabad
	West Sabzevaran_ South Faryab
	West Sabzevaran_ North Kahnuj
	Main Zagros Reveres_ Chahmazrae
	North Jebale Barez_ Gowk
Triple	Main Zagros Reveres_ North Faryab-Zendan Minab Palami
Cutting (Crossing)	Bam_ Dehno
	Dehbakri_ South Jebal-e Barez
Mutually cutting (Crossing)	West Sabzevaran_ Chahmazrae_ South Jebal-e Barez
Relay	Bam_ Gowk
	Gowk_ Dehbakri
	Dehbakri_ East Sabzevaran
	Dehbakri_ West Sabzevaran
	West Sabzevaran_ Gowk
	West Sabzevaran_ Bam
	West Sabzevaran_ Jiroft
Arrays	Segments of the Chahmazrae
	Segments of the North Faryab
	Segments of the East Sabzevaran
	Segments of the Jiroft
	Jiroft_ East Sabzevaran
	Jiroft_ East Sabzevaran-Dehbakri-Gowk
Intersection line parallel to displacement	North Jebal-e Barez_ Gowk
Intersection line approximately normal to displacement	West Sabzevaran_ North Kahnuj
	West Sabzevaran_ Chahmazrae
Intersection line normal to displacement and parallel to displacement	Bam_ Dehno
	Dehbakri_ South Jebal-e Barez
	West Sabzevaran_ South Jebal-e Barez
	West Sabzevaran_ Heydarabad
	West Sabzevaran_ South Faryab
Different displacement directions	West Sabzevaran_ Chahmazrae_ South Jebal-e Barez
Antithetic	Suru_ Hojatabad_ South Jebal-e Barez with Dehno_ North Jebal-e Barez
	West Sabzevaran_ Chahmazrae
	West Sabzevaran_ North Faryab
	West Sabzevaran_ North Kahnuj
Synthetic	Suru_ Hojatabad_ South Jebal-e Barez
	Dehno_ North Jebal-e Barez
	West Sabzevaran_ Dehpish
	East Sabzevaran_ Dehpish
Neutral intersection	North Jebal-e Barez_ Gowk
Extensional Y	Suru_ Hojatabad_ South Jebal-e Barez With Dehno_ North Jebal-e Barez
Contractional Y	West Sabzevaran_ Chahmazrae
	West Sabzevaran_ North Kahnuj
Trailing	Bam_ Dehno

fractures. In the study area, the faults in some area hardly behave independently but as a sets or networks, where the adjustment of these faults cause a variety of different fault interactions. We determined the kinematic, geometric, topological relationships between faults in the study area and concentrated on how these faults have formed networks (Tables 2 and 3).

Shear fractures propagate a short distance out of the main fault.

Table 3
Structural zones in the study area.

Type of structural zones	Faults
Strike Slip Zone	West Sabzevaran
	Jiroft_ East Sabzevaran_ Dehbakri_ Gowk
	Bam
	Chahmazrae
	Faryab
Compressional Zone	Bam_ Gowk
	Bam_ Dehbakri
Extensional Zone (Pull-apart)	Bam_ East Sabzevaran
	Bam_ West Sabzevaran
	Dehbakri_ East Sabzevaran
	Dehbakri_ West Sabzevaran
Simple Shear Zone	North Faryab_ Chahmazrae
	West Sabzevaran_ East Sabzevaran
	West Sabzevaran_ Jiroft
Imbricate Zone	Heydarabad_ South Faryab
	Suru_ Hojatabad_ South Jebal-e Barez
	Dehno_ North Jebal-e Barez
Flower Structural Zone	Dehno_ North Jebal-e Barez_ South Jebal-e Barez_ Hojatabad_ Suru

Riedel shear is also used on a large-scale fault pattern and may refer to three direction of associated fractures (R, P, and R′). Its individual fractures remain active after the other types developed. Therefore, the synchronous movements on the all fractures determine the strain in the fault zone. The geometrical arrangement of the Riedel shears is indicative of the sense of movement within the wrench zone and is therefore widely used for the interpretation of its kinematic evolution. The Sabzevaran fault system, the N–S right-lateral strike-slip fault (length over 300 km), is located in the middle of the study area (Fig. 2). It propagated the deformation by partitioning of dip-slip and strike-slip components on its branches (Fig. 2). The geometrical relationship between these sets and their shear sense demonstrates the assemblage of the Riedel shear fractures. Fault-related fractures are different sets developing at a special angle to main fault. In the North Faryab city, between North Faryab and Chahmazrae faults, Riedel shears are well developed. In this area, our proposed tectonic model is transpressional zone, with high seismic activity (Figs. 13 and 14). For example, the March 4, 1999 Faryab earthquake (Mw6.6) and its aftershocks were located inside this transpressional zone (marked by no. 9 in Table 4 and Fig. 13). The North Faryab and Chahmazrae faults in the southwestern part approach to the MZRF (Fig. 2). This interaction is very young, so that we can see the uplift of Pliocene rock units (Fig. 14b). It is close to the February 28, 2006 Tiab earthquake (Fig. 14) and therefore, it could be causal fault of that earthquake.

In the Chahmazrae-Faryab shear zone two clusters of earthquakes are observed. Events near the MZRF have generally depth less than the cluster which is located far from the fault (Fig. 14). Regarding to ~ NE dipping of MZRF in shear zone, it can be suggested that both clusters occurred in response to the shear at different depths.

An earthquake may propagate from one fault to the next one and it depends on how strongly the faults are interacting. Interaction ranges from faults that are mechanically independent to those linked so strongly as to be acting as a single mechanical unit. Similarly, there is no simple distinction between interacting faults and segments of a single fault. For example, the three primary faults ruptured in the Landers earthquake (June 28, 1992) in the western United States (see Hill et al., 1993; Sieh et al., 1993); the two segments of Gowk fault ruptured in the five Gowk earthquakes (1981–1998) (see Berberian, 2001); some segments of North Anatolian fault, Turkey, ruptured in ten earthquakes, which occurred between 1939 and 1992 (Yamamoto et al., 2017; Stein et al., 1997). There are also some examples that show one fault can activate another fault at their intersection. For example Dashte-e Bayaz and Zirkuh earthquake sequences in eastern Iran, occurred by two faults with different strike (Walker et al., 2011); the conjugate faults were the reason of the two Rigan earthquakes in southeast Iran (Walker et al.,

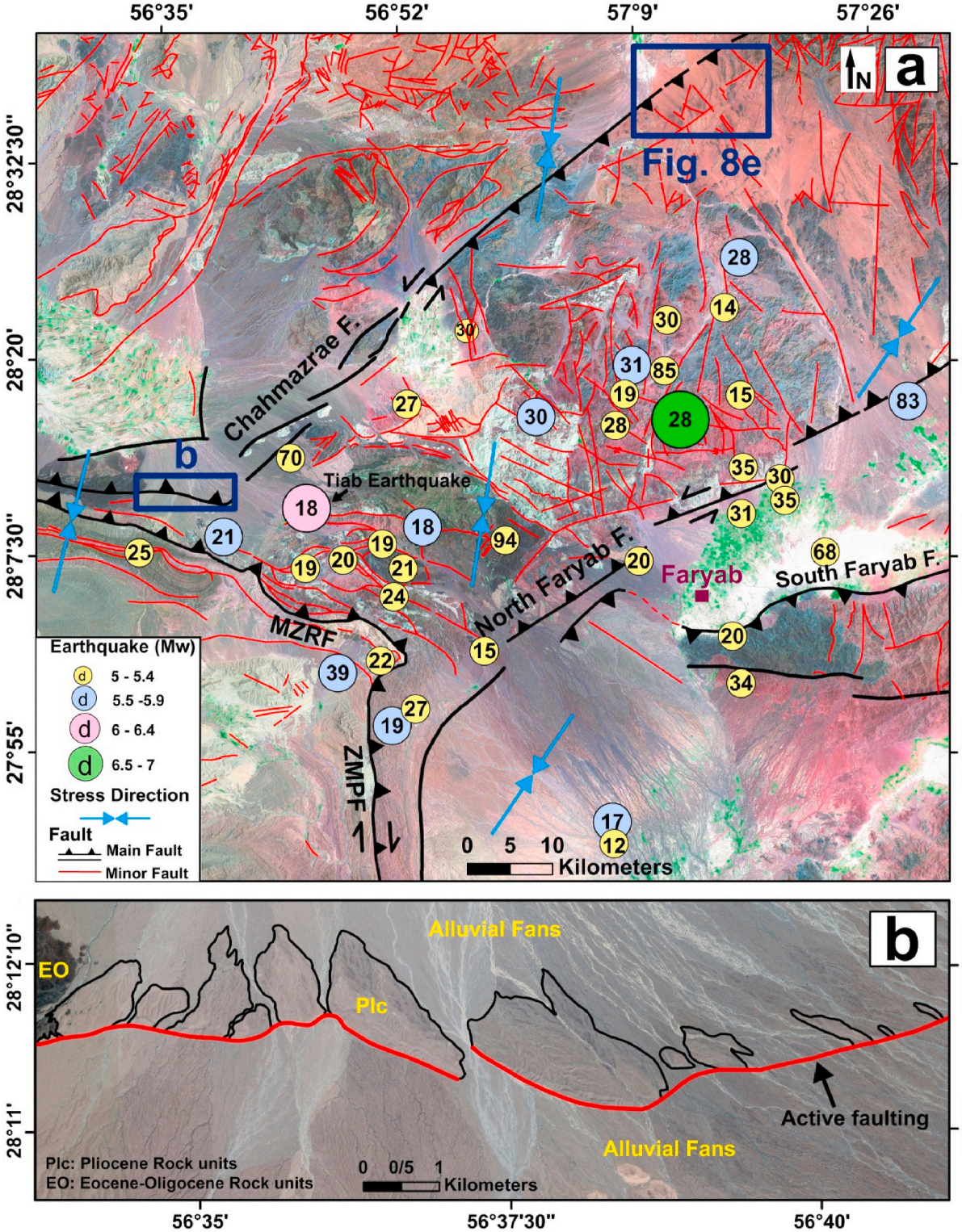

Fig. 14. a) The faults and the earthquakes in the southwestern part of the study area. The numbers in the circles are the earthquakes depth (d), Stress directions are from Zarifi et al. (2014). b) Uplift of Pliocene rock units at interaction of Chahmazrae and MZRF zone. ZMPF= Zendan-Minab-Palami Fault, MZRF= Main Zagros Reverse Fault.

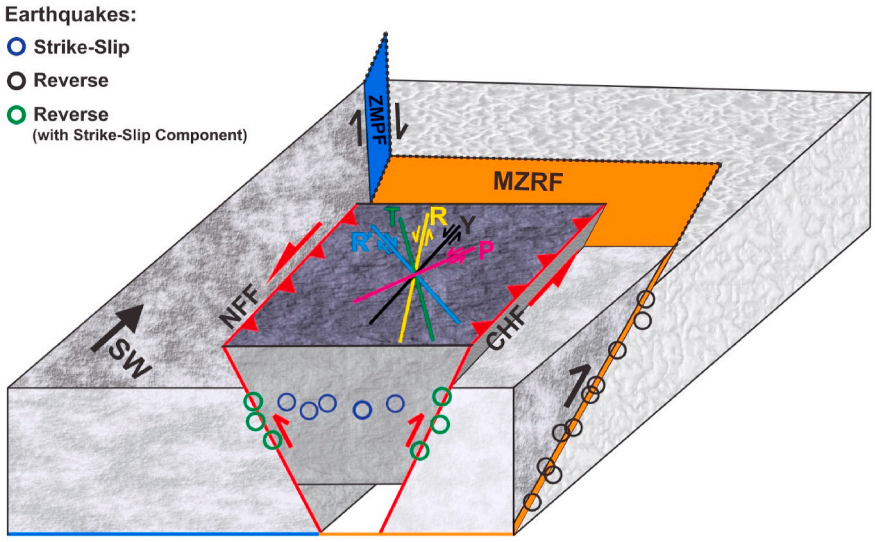

Fig. 15. The 3-D schematic diagram of the faults and earthquakes in the southwestern part of the study area. MZRF = Main Zagros Reverse Fault, CHF= Chahmazrae, NFF=North Faryab Fault, ZMPF = Zendan-Minab-Palami Fault.

Table 4
The earthquake source parameters in the study area. The labels in the last column refer to the focal mechanisms shown in Fig. 13. CMT= Centroid Moment Tensor, Harvard University, United States of America; IIEES= International Institute of Earthquake Engineering and Seismology, Iran; IRSC= Iranian Seismological Center; EHB= Engdahl et al. (2006); M97= Mirzaei et al. (1997).

Date (month/day/year)	Time	Lat. (°N)	Lon. (°E)	Mag. (Mw)	Depth (Km)	Ref.	Label
		From: IIEES, and IRSC					
12/26/2003	01:56:00	28.95	58.26	6.6	13 (IIEES)	CMT	1
07/22/2004	04:51:39	29.11	58.24	4.7	17.2	CMT	2
June 10, 2004	11:14:31	28.75	57.93	5.2	14 (IIEES)	CMT	3
11/16/2018	20:17:05	27.95	58.29	5.1	100 (IRSC)	CMT	4
04/18/2012	17:40:42	27.76	57.96	5.1	60 (IRSC)	CMT	5
July 03, 2018	14:46:12	28.035	57.746	5.4	28 (IRSC)	CMT	6
10/20/1997	06:09:09	28.443	57.278	5.4	28 (EHB)	CMT	7
July 10, 2004	12:54:59	28.39	57.26	5.0	14 (IIEES)	CMT	8
April 03, 1999	05:38:34	28.271	57.207	6.6	28 (EHB)	CMT	9
February 04, 1989	06:42:09	28.171	57.28	5.3	31 (EHB)	CMT	10
May 03, 2011	20:42:52	28.298	57.14	5.2	20 (IRSC)	CMT	11
December 04, 1993	14:00:52	28.265	57.129	4.9	28 (EHB)	CMT	12
02/26/1996	08:08:23	28.274	57.034	5.5	30 (EHB)	CMT	13
12/22/1964	04:36:35	28.157	56.898	5.4	42	M97	14
May 03, 2015	22:54:50	28.055	56.959	4.9	16	IRSC	15
02/28/2006	07:32:04	28.18	56.76	6.0	18	IIEES	16
12/19/1991	18:55:21	28.041	57.269	5.4	20 (EHB)	CMT	17
September 05, 2014	00:08:45	27.903	57.520	4.7	40	IRSC	18
February 06, 2014	22:51:17	27.838	57.370	4.6	32	IRSC	19
10/24/2014	12:38:56	27.772	57.400	4.8	24	IRSC	20
10/23/2017	00:24:17	27.844	57.125	5.4	17.6 (IRSC)	CMT	21
October 11, 2010	13:49:12	27.773	57.041	4.9	29 (IRSC)	CMT	22

2013) and three faults were caused by the 1927 Tongo, 1943 Tottori, and 2000 Tottori-ken earthquakes sequences in Japan (Ishibe et al., 2011).

Our investigations provide a framework to analyze the interacting faults based on their geometric and kinematic relationships, which can have potentially some implications for similar tectonic settings around the world. To give some examples, we can refer to faults in the San Francisco Bay region of California (Aydin and Page., 1984), faults in Eastern Himalayan Syntaxis (EHS) around the indentor (Peter et al., 2018; Gupta et al., 2015), Moab fault and its branches in southern Utah (Fossen et al., 2005) and Mariánské-Lázně fault in the West Bohemia Swarm Region, Czech Republic (Vavryčuk and Adamová., 2018).

8. Conclusions

Our neotectonic and morphotectonic studies helped us to identify most of the potentially active faults in the Sabzevaran area. The active seismogenic faults cut the Quaternary sediments and can be detected on the aerial photographs and the satellite images. The activity of some faults such as the Sabzevaran, North Faryab, Chahmazrae, and Jebal-Barez can potentially cause some earthquakes on other faults. We found out that there is an increment in the fault scarps height from the west to the east toward the center, where the intersections are placed.

We suggested the type of fault interactions, by field observations and geomorphological analysis (Table 2). These types of the fault interactions demonstrate how a possible earthquake, in the Sabzevaran area, may propagate from one fault to the next. We also determined the types of structural zones coexisting with each other in the area (Table 3).

Table 5
The earthquake source parameters in the SW study area. NOW= Nowroozi (1985); ISC= International Seismological Centre, United Kingdom; EHB= Engdahl et al. (2006); IIEES= International Institute of Earthquake Engineering and Seismology, Iran; IRSC= Iranian Seismological Center, mb= Body-Wave Magnitude, Mw= Moment Magnitude, ML= Local Magnitude, MN= Nuttli Magnitude (Nuttli, 1973).

ID	Date (month/day/year)	Time	Lat. (°N)	Lon. (°E)	Mag.	Mag. Type	Depth (km)	Ref.
1	09/29/1962	06:54:00	28.29	57.48	5.5	mb	83	NOW
2	November 05, 1964	06:07:41	28.13	57.38	5.3	mb	68	ISC
3	12/22/1964	04:36:34	28.157	56.898	5.7	mb	18	EHB
4	12/23/1964	10:52:24	28.23	56.74	5.0	mb	70	ISC
5	August 11, 1965	01:57:26	27.964	56.89	5.1	mb	27	EHB
6	January 03, 1967	10:12:48	28.083	56.864	5.1	mb	24	EHB
7	12/20/1971	23:27:43	28.323	57.188	5.0	mb	85	ISC
8	March 04, 1972	09:07:14	28.121	57.157	5.0	mb	20	EHB
9	February 08, 1972	23:03:29	28.122	56.803	5.0	mb	20	EHB
10	April 11, 1972	09:32:26	28.143	56.997	5.0	mb	94	ISC
11	08/25/1973	14:58:08	28.113	56.758	5.3	mb	19	EHB
12	11/13/1976	10:12:34	28.208	57.326	5.0	mb	30	EHB
13	02/22/1978	20:18:00	28.113	56.875	5.0	mb	21	EHB
14	02/23/1978	23:24:50	28.139	56.85	5.1	mb	19	EHB
15	June 01, 1981	07:23:40	28.129	56.559	5.0	mb	25	EHB
16	10/15/1982	02:53:52	28.185	57.332	5.0	mb	35	EHB
17	07/25/1986	10:08:07	27.991	57.279	5.2	mb	34	EHB
18	12/18/1987	16:24:04	28.146	56.66	5.9	Mw	21	EHB
19	September 06, 1988	12:09:50	28.29	56.88	5.2	Mw	27	EHB
20	February 04, 1989	06:42:04	28.171	57.28	5.4	Mw	31	EHB
21	12/19/1991	18:55:18	28.041	57.269	5.4	Mw	20	EHB
22	December 04, 1993	14:00:41	28.265	57.129	5.2	mb	28	EHB
23	02/26/1996	08:08:20	28.274	57.034	5.5	Mw	30	EHB
24	04/19/1997	05:53:14	27.946	56.862	5.6	Mw	19	EHB
25	10/20/1997	06:09:05	28.443	57.278	5.5	mb	28	EHB
26	April 03, 1999	07:26:05	28.365	56.951	5.0	mb	30	EHB
27	April 03, 1999	09:52:03	28.377	57.191	5.1	mb	30	EHB
28	April 03, 1999	05:47:51	28.329	57.149	5.5	mb	31	EHB
29	April 03, 1999	05:38:27	28.271	57.207	6.6	Mw	28	EHB
30	May 03, 2000	09:40:06	27.933	56.451	5.4	mb	25	EHB
31	11/25/2001	21:30:55	28.22	57.282	5.1	Mw	35	EHB
32	02/14/2003	10:29:00	28.002	56.797	5.6	Mw	39	EHB
33	July 10, 2004	12:54:56	28.39	57.26	5.0	ML	14	IIEES
34	02/28/2006	07:32:04	28.18	56.76	6.0	Mw	18	IIEES
35	May 03, 2011	12:42:53	28.298	57.14	5.1	MN	19.3	IRSC
36	May 03, 2015	02:54:49	28.055	56.959	5.2	MN	15.7	IRSC
37	08/31/2017	01:30:27	27.821	57.127	5.4	MN	12.1	IRSC
38	10/23/2017	12:24:14	27.844	57.125	5.5	MN	17.6	IRSC
39	01/22/2020	09:23:15	28.015	56.848	5.2	MN	22.4	IRSC
40	03/27/2020	06:40:43	28.297	57.279	5.4	MN	15.1	IRSC

It helped us to better understand the geometrical and kinematical relationship between different fault sets.

Our investigation suggests that the Dehbakri and Gowk faults are continuation of the Jiroft and East Sabzevaran faults in the Jiroft plain. The geometrical relationship between these fault systems are relay interactions. These fault systems with right-step arrangement created several pull-apart basins. The geometry and kinematics of these faults in the Jebal-e Barez Mountains suggest a positive flower structure.

In the North of Faryab city, between the North Faryab and Chahmazrae faults, a shear zone was recognized and presented. In this area, our proposed model is a transpressional zone, with high seismic activity. We suggest that MZRF is the source of reverse events and the Chahmazrae-Faryab shear zone is the source of left-lateral, oblique reverse faulting events, and strike-slip events. These types of the earthquakes in the study area confirm the idea of tectonic proximity of the root faults and shear zones.

Declaration of competing interest

The authors declare that they have no known competing financial interests or personal relationships that could have appeared to influence the work reported in this paper.

Acknowledgements

This work was supported by International Institute of Earthquake Engineering and Seismology (IIEES). We are grateful to the editor, Toru Takeshita, for his useful comments on the manuscript. We also thank two anonymous reviewers for their constructive and detailed reviews and Holger Stuenitz for improving the previous version of this manuscript.

References

Agard, P., Omrani, J., Jolivet, L., Mouthereau, F., 2005. Convergence history across Zagros (Iran): constraints from collisional and earlier deforma-tion. Int. J. Earth Sci. 94, 401–419.

Agard, P., Monie, P., Gerber, W., Omrani, J., Molinaro, M., Meyer, B., Labrousse, L., Vrielynck, B., Jolivet, L., Yamato, P., 2006. Transient syn-obduction exhumation of Zagros blue schists inferred from P-T-deformation-time-kinematics constraints: implications for the Neotethyan wedge dynamics. J. Geophys. Res. 111, B11401.

Agard, P., Omrani, J., Jolivet, L., Whitechurch, H., Vrielynck, B., Spakman, W., Monié, P., Meyer, B., Wortel, R., 2011. Zagros orogeny: a subduction-dominated process. Geol. Mag. 148, 692–725. https://doi.org/10.1017/S001675681100046X.

Aghanabati, A., Eftekhar Nezhad, J., Samimi Namin, M., Arshadi, S., 1993. Geological Map of Bam, scale 1:100,000. Geol. Surv. Iran.

Allmendinger, R.W., Gephart, J.W., Marrett, R.A., 1989. Notes on Fault Slip Analysis. Geological Society of America, p. p56.

Aubourg, C., Smith, B., Bakhtari, H., Guya, N., Eshragi, A., Lallemant, S., Molinaro, M., Braud, X., Delaunay, S., 2004. Post-miocene Shortening Pictured by Magnetic Fabric across the Zagros-Makran Syntaxis (Iran), vol. 383. Geological Society of America special paper, pp. 17–40.

Aydin, A., Page, B.M., 1984. Diverse Pliocene-Quaternary Tectonics in a Transform Environment, San Francisco Bay Region, California, vol. 95. Geological Society of America Bulletin, pp. 1303–1317.

Babakhani, N., Alavi Tehrani, N., 1992. Geological Map of Sabzevaran, scale 1:250,000. Geol. Surv. Iran.

Bastesen, E., Rotevatn, A., 2012. Evolution and structural style of relay zones in layered limestone–shale sequences: insights from the Hammam Faraun Fault Block, Suez rift, Egypt. J. Geol. Soc. 169, 477–488. London.
Berberian, F., Berberian, M., 1981. Tectono-plutonic episodes in Iran. In: Gupta, H.K., Delany, F.M. (Eds.), Zagros-Hindu Kush-Himalaya Geodynamic Evolution, Am. Geophys. Union, Geodynamics Series, vol. 3, pp. 5–32.
Berberian, M., Papastamatiou, D., 1978. Khurgu (North Bandar Abbas, Iran) earthquake of March 21, 1977; a preliminary field report and a seismotectonic discussion. Bull. Seismol. Soc. Am. 68, 411–428.
Berberian, F., Muir, I.D., Pankhurst, R.J., Berberian, M., 1982. Late cretaceous and early miocene andean-type plutonic activity in northern makran and Central Iran. J. Geol. Soc. 139, 605–614.
Berberian, M., Jackson, J.A., Fielding, E., Parsons, B.E., Priestly, K., Qorashi, M., Talebian, M., Walker, R., Wright, T.J., Baker, E., 2001. The 1998 March 14 Fandoqa earthquake (Mw 6.6) in Kerman, southeast Iran: re-rupture of the 1981 Sirch earthquake fault, triggering of slip on adjacent thrusts, and the active tectonics of the Gowk fault zone. Geophys. J. Int. 146 (2), 371–398.
Blanc, E.J.-P., Allen, M.B., Inger, S., Hassani, H., 2003. Structural styles in the Zagros simple folded zone, Iran. J.Geol. Soc. Lond. 160, 401–412.
Bourne, S.J., Willemse, E.J.M., 2001. Elastic stress control on the pattern of tensile fracturing around a small fault network at Nash Point. J. Struct. Geol. 23, 1753–1770.
Bull, J.M., Barnes, P.M., Lamarche, G., Sanderson, D.J., Cowie, P.A., Taylor, S.K., Dix, J. K., 2006. High-resolution record of displacement accumulation on an active normal fault: implications for models of slip accumulation during repeated earthquakes. J. Struct. Geol. 28, 1146–1166.
Burge, J.P., 2018. Geology of the onshore Makran accretionary wedge: synthesis and tectonic interpretation. Earth Sci. Rev. 185, 1210–1231.
Byrne, D.E., Sykes, L.R., Davis, D.M., 1992. Great thrust earthquakes and aseismic slip along the plate boundary of the Makran subductionzone. J. Geophys. Res. 97 (B1), 449–478.
Choi, J.H., Edwards, P., Ko, K., Kim, Y.S., 2016. Definition and classification of fault damage zones: a review and a new methodological approach. Earth Sci. Rev. 152, 70–87.
Derakhshani, R., Eslami, S., 2011. A new view point for seismotectonic zoning. Am. J. Environ. Sci. 7, 212–218. https://doi.org/10.3844/ajessp.2011.212.218.
Derakhshani, R., Farhoudi, G., 2005. Existence of the Oman line in the empty quarter of Saudi Arabia and its continuation in the red sea. J. Appl. Sci. 5, 745–752 **(Error! Hyperlink reference not valid.**.
Dooley, T.P., Schreurs, G., 2012. Analogue modelling of intraplate strike-slip tectonics: a review and new experimental results. Tectonophysics 574–575, 1–71.
Duffy, O.B., Bell, R.E., Jackson, C.A.L., Gawthorpe, R.L., Whipp, P.S., 2015. Fault growth and interactions in a multiphase r if fault network: the Horda Platform, Norwegian North Sea. J. Struct. Geol. 80, 99–119.
Edey, A., Allen, M.B., Nilfouroushan, F., 2020. Kinematic variation within the Fars Arc, eastern Zagros, and the development of fold-and-thrust belt curvature. Tectonics. https://doi.org/10.1029/2019TC005941.
Engdahl, E.R., Jackson, J.A., Myers, S.C., Bergman, E.A., Priestley, K., 2006. Relocation and assessment of seismicity in the Iran region. Geophys. J. Int. 167, 761–778.
Fattahi, m., Walker, R.T., Talebian, M., Solan, R.A., Rasheedi, A., 2014. LateQuaternary active faulting and landscape evolution in relation to theGowk Fault in the South Golbaf Basin, S.E. Iran. Geomorphology 204, 334–343.
Fielding, E.J., Talebian, M., Rosen, P.A., Nazari, H., Jackson, J.A., Ghorashi, M., Walker, R., 2005. Surface ruptures and building damage of the 2003 Bam, Iran earthquake mapped by satellite synthetic aperture radar interferometric correlation. J. Geophys. Res. 110, JB003299.
Fossen, H., Rotevatn, A., 2016. Fault linkage and relay structures in extensional settings - a review. Earth Sci. Rev. 154, 14–28.
Fossen, H., Johansen, T.E.S., Hesthammer, J., Rotevatn, A., 2005. Fault interaction in porous sandstone and implications for reservoir management; examples from southern Utah. AAPG (Am. Assoc. Pet. Geol.) Bull. 89, 1593–1606.
Frankowicz, E., McClay, K.R., 2010. Extensional fault segmentation and linkages, bonaparte basin, outer north west shelf, Australia. AAPG (Am. Assoc. Pet. Geol.) Bull. 94, 977–1010.
Fu, B., Lei, X., Hessami, K., Ninomiya, Y., Azuma, T., Kondo, H., 2007. A new fault rupture scenario for the 2003 Mw 6.6 Bam earthquake, SE Iran: insights from the high-resolution QuickBird imagery and field observations. J. Geodyn. 44, 160–172.
Gawthorpe, R.L., Jackson Young, C.A.L.M.J., Sharp, I.R., Moustafa, A.R., Leppard, C.W., 2003. Normal fault growth, displacement localisation and the evolution of normal fault populations: the Hammam Faraun fault block, Suez rift, Egypt. J. Struct. Geol. 25, 883–895.
Gholamzadeh, A.F., Yamini-Fard, F., Hessami, K., Tatar, M., 2009. The February 28, 2006 Tiab earthquake, Mw 6.0: implications for tectonics of the transition between the Zagros continental collision and the Makran subduction zone. J. Geodyn. 47 (5), 280–287.
Gholamzadeh, A., Rahimi, H., Yaminifard, F., 2014. Spatial and temporal variation of coda-wave attenuation in the Faryab region, southeast of the sanandaj–sirjan zone, using aftershocks of the Tiab earthquake of 28 february 2006. Bull. Seismol. Soc. Am. 104 (1), 529–539. https://doi.org/10.1785/0120130072.
Gupta, T.D., Riguzzi, F., Dasgupta, S., Mukhopadhyay, B., Roy, S., Sharma, S., 2015. Kinematics and strain rates of the eastern himalayan syntaxis from new GPS campaigns in northeast India. Tectonophysics 655, 15–26. https://doi.org/10.1016/j.tecto.2015.04.017.
Hessami, K., Nilforoushan, F., Talbot, C.J., 2006. Active deformation within the Zagros mountains deduced from GPS measurements. J. Geol. Soc. London 163, 143–148..
Hessami, K., Mobayyen, F., Tabassi, H., 2013. The Map of Active Faults of Iran. International institute of earthquake engineering and seismology, Tehran.
Hill, D.P., Reasenberg, P.A., Michael, A., Arabaz, W.J., Beroza, G., Brumbaugh, D., Brune, J.N., Castro, R., Davis, S., dePolo, D., Ellsworth, W.L., Gomberg, J., Harmsen, S., House, L., Jackson, S.M., Johnston, M.J.S., Jones, L., Keller, R., Malone, S., Munguia, L., Nava, S., Pechmann, J.C., Sanford, A., Simpson, R.W., Smith, R.B., Stark, M., Stickney, M., Vidal, A., Walter, S., Wong, V., Zollweg, J., 1993. Seismicity remotely triggered by the magnitude 7.3 Landers, California, earthquake. Science 260, 1617–1623.
Ishibe, T., Shimazaki, K., Tsuruoka, H., Yamanaka, Y., Satake, K., 2011. Correlation between Coulomb stress changes imparted by large historical strike-slip earthquakes and current seismicity in Japan. Earth Planets Space 63, 301–314.
Jackson, M., Bouchon, M., Fielding, E., Funning, G., Ghorashi, M., Hatzfeld, D., Nazari, H., Parsons, B., Priestley, K., Talebian, M., Tatar, M., Walker, R., Wright, T., 2006. Seismotectonic, rupture process, and earthquake-hazard aspects of the 2003 December 26 Bam, Iran, earthquake. Geophys. J. Int. 166, 1270–1292.
Jentzer, M., Fournier, M., Agard, P., Omrani, J., Khatib, M.M., Whitechurch, H., 2017. Neogene to Present paleostress field in Eastern Iran (Sistan belt) and implications for regional geodynamics. Tectonics 36, 321–339. https://doi.org/10.1002/2016TC004275.
Kattenhorn, S.A., Aydin, A., Pollard, D.D., 2000. Joints at high angles to normal fault strike: an explanation using 3-D numericalmodels of fault-perturbed stress fields. J. Struct. Geol. 22, 1–23.
Khodaverdian, A., Zafarani, H., Rahimian, M., 2015. Long term fault slip rates, distributed deformation rates and forecast of seismicity in the Iranian Plateau. Tectonics 34, 2190–2220. https://doi.org/10.1002/2014TC003796.
Khorrami, F., Vernant, P., Masson, F., Nilfouroushan, F., Mousavi, Z., Nankali, H., Saadat, S., Walpersdorf, A., Hosseini, S., Tavakoli, P., Aghamohammadi, A., Alijanzade, 2019. An up-to-date crustal deformation map of Iran using integrated campaign-mode and permanent GPS velocities. Geophys. J. Int. 217 (2), 832–843.
Kim, Y.S., Peacock, D.C.P., Sanderson, D.J., 2004. Fault damage zones. J. Struct. Geol. 26, 503–517.
Kopp, C., Fruehn, J., Flueh, E.R., Reichert, C., Kukowski, N., Bialas, J., Klaeschen, D., 2000. Structure of the Makran subduction zone from wide angle and reflection seismic data. Tectonophysics 329, 171–191.
Leeder, M.R., Jackson, J.A., 1993. The interaction between normal faulting and drainage in active extensional basins, with examples from the western United States and central Greece. Basin Res. 5, 79–102.
Maerten, L., Gillespie, P., Pollard, D.D., 2002. Effects of local stress perturbation on secondary fault development. J. Struct. Geol. 24, 145–153.
Nilforoushan, F., Masson, F., Vernant, P., Vigny, C., Martinod, J., Abbassi, M., Nankali, H., Hatzfeld, D., Bayer, R., Tavakoli, F., Ashtiani, A., Doerflinger, E., Daignières, M., Collard, P., Chéry, J., 2003. GPS network monitors the Arabia-Eurasia collision deformation in Iran. J. Geodes. 77, 411–422.
Masson, F., Chéry, J., Hatzfeld, D., Martinod, J., Vernant, P., Tavakoli, F., Ghafory-Ashtiani, M., 2005. Seismic versus aseismic deformation in Iran inferred from earthquakes and geodetic data. Geophys. J. Int. 160, 217–226.
McCall, G.J.H., 1997. The geotectonic history of the Makran and adjacent areas of southern Iran. J. Asian Earth Sci. 15 (6), 517–531.
McCall, G.J.H., Kidd, R.G.W., 1982. The Makran, southeastern Iran: the anatomy of a convergent plate margin active from Cretaceous to present. In: Leggett, J.K. (Ed.), Trench-forearc Geology: Sedimentation and Tectonics on Modern and Ancient Active Plate Margins, vol. 10. Geological Society of London Special Publication, Oxford, pp. 387–397. Blackwell Scientific.
McCall, G.J.H., Morgan, K.H., Campe, G.C., Child, R., Porter, D.J., Wyatt, J.D., Bailey, P. B.H., Craik, D.I., Dalaei, H., Jones, D., McCormick, C.D., Motamedi, S., Nunn, G.A.G., Pooyai, N., Power, P., Smith, G.H., Swain, C.R., Simonian, K., Deighton, I., Mallett, C.W., Huber, H., Peterson, L.W., Rudzinskas, K.K., Samimi Namin, M., Hadji Zad-Kabir, Y., 1985. Minab Quadrangle Map 1:250,000 and Explanatory Text. Geological Survey of Iran, p. 534.
Meyer, B., Le Dortz, K., 2007. Strike-slip kinematics in Central and Eastern Iran: estimating fault slip-rates averaged over the Holocene. Tectonics 26, TC5009. https://doi.org/10.1029/2006TC002073.
Mirzaei, N., Gao, M., Chen, Y.T., Wang, J., 1997. A uniform catalog of earthquakes for seismic hazard assessment in Iran. Acta Seismol. Sin. (Engl. Ed.) 10, 713–726.
Nemati, M., 2015. Aftershocks investigation of 2010 Dec. and 2011 Jan. Rigan earthquakes in the southern Kerman province, SE Iran. J. Tethys 3 (2), 97–114.
Nemati, M., Jafari Hajati, F., Rashidi, A., Hassanzadeh, R., 2020. Seismology of the 2017 hojedk earthquakes (MN6.0–6.1), kerman province, SE Iran. Tectonophysics 780, 228–398.
Nixon, C.W., Sanderson, D.J., Dee, S., Bull, J.M., Humphreys, R., Swanson, M., 2014. Fault interactions and reactivation within a normal fault network at Milne Point, Alaska. AAPG (Am. Assoc. Pet. Geol.) Bull. 98, 2081–2107.
Nowroozi, A., 1985. Empirical relations between magnitude and fault parameters for earthquakes in Iran. Bull. Seismol. Soc. Am. 75 (5), 1327–1338.
Peacock, D.C.P., Sanderson, D.J., 1991. Displacements, segment linkage and relay ramps in normal fault zones. J. Struct. Geol. 13, 721–733.
Nuttli, O. W, 1973. Seismic wave attenuation and magnitude relations for eastern North America. Journal of Geophysical Research 78 (5), 876–885. https://doi.org/10.1029/JB078i005p00876.
Peacock, D.C.P., Nixon, C.W., Rotevatn, A., Sanderson, D.J., Zuluaga, L.F., 2016. Glossary of fault and other fracture networks. J. Struct. Geol. 92, 12–29.
Peacock, D.C.P., Nixon, C.W., Rotevatn, A., Sanderson, D.J., Zuluaga, L.F., 2017. Interacting faults. J. Struct. Geol. 97, 1–22.

Peter, J.H., Andrew, V.Z., An, Y., 2018. West-directed thrusting south of the eastern Himalayan syntaxis indicates clockwise crustal flow at the indenter corner during the India-Asia collision. Tectonophysics 722, 277–285.
Peyret, M., Djamour, Y., Hessami, K., Regard, V., Bellier, O., Vernant, P., Daignieres, M., Nankali, H., Van Gorp, S., Goudarzi, M., Chery, J., Bayer, R., Rigoulay, M., 2009. Present-day strain distribution across the Minab-Zendan-Palami fault system from dense GPS transects. Geophys. J. Int. 179, 751–762.
Raeesi, M., Zarifi, Z., Nilfouroushan, F., Boroujeni, S.A., Tiampo, K., 2017. Quantitative analysis of seismicity in Iran. Pure Appl. Geophys. 174, 793–833.
Rashidi Boshrabadi, A., Khatib, M.M., Raeesi, M., Mousavi, S.M., Djamour, Y., 2018. Geometric-kinematic characteristics of the main faults in the W-SW of the Lut Block (SE Iran). J. Afr. Earth Sci. 139, 440–462. https://doi.org/10.1016/j.jafrearsci.2017.12.027.
Rashidi, A., Khatib, M.M., Mosavi, S.M., Jamor, Y., 2017. Estimation of the active faults, based on Seismic, geologic and geodetic moment rates in the South and West of Lut block. J. Geosci. 26, 211–222. https://doi.org/10.22071/gsj.2017.50265.
Rashidi, A., Khatib, M.M., Nilfouroushan, F., Derakhshani, R., Mousavi, S.M., Kiyani, H., Jamour, Y., 2019. Strain rate and stress fields in the West and South Lut block, Iran: insights from the inversion of focal mechanism and geodetic data. Tectonophysics 766, 94–114.
Regard, V., Bellier, O., Thomas, J.-C., Abbassi, M.R., Mercier, J., Shabanian, E., Fegghi, K., Soleymani, S., 2004. The accommodation of Arabia– Eurasia convergence in the Zagros-Makran transfer zone, SE Iran: a transition between collision and subduction through a young deforming system. Tectonics 23, TC4007. https://doi.org/10.1029/2003TC001599.
Regard, V., Bellier, O., Thomas, J.-C., Bourlès, D., Bonnet, S., Abbassi, M.R., Braucher, R., Mercier, J., Shabanian, E., Soleymani, Sh, Feghhi, Kh, 2005. Cumulative right-lateral fault slip rate across the Zagros-Makran transfer zone: role of the Minab-Zendan fault system in accommodation Arabia-Eurasia convergence in southeast Iran. Geophys. J. Int. 162, 177–203.
Regard, V., Bellier, O., Braucher, R., Gasse, F., Bourlès, D.L., Mercier, J.L., Thomas, J.-C., Abbassi, M.R., Shabanian, E., Soleymani, S., 2006. ^{10}Be dating of alluvial deposits from Southeastern Iran (the Hormoz Strait area). Palaeogeogr. Palaeoclimatol. Palaeoecol. 242, 36–53.
Regard, V., Hatzfeld, D., Molinaro, M., Aubourg, C., Bayer, R., Yamini-Fard, F., Petrite, M., Abbassi, M., 2009. The transition between Makran subduction and the Zagros collision: recent advances in its structure and active deformation. Geological Society, London, Special Publications 330 (1), 43–65, 43.
Rodgers, D.A., 1980. Analysis of pull-apart basin development produced by en échelon strike-slip faults. In: Balance, P.F., Reading, H.G. (Eds.), Sedimentation in Oblique-Slip Mobile Zones, vol. 4. International Association of Sedimentologists Special Publication, pp. 27–41.
Ross, D.A., Uchupi, E., White, R.S., 1986. The geology of the Persian gulf-gulf of Oman region: a synthesis. Rev. Geophys. 24, 537–556.
Savidge, E., Nissen, E., Nemati, M., Karasozen, E., Hollingsworth, J., Talebian, M., Bergman, E., Ghods, A., Ghorashi, M., Kosari, E., Rashidi, A., Rashidi, A., 2019. The December 2017 Hojedk (Iran) earthquake triplet- sequential rupture of shallow reverse faults in a strike-slip restraining bend. Geophys. J. Int. 217, 909–925.
Shafiei, S.H., Mohajjel, M., 2015. Structural evidence for slip partitioning and inclined dextral transpression along the SE Sanandaj–Sirjan zone, Iran. Int. J. Earth Sci. 104, 587–601.
Shafiei, S.H., Alavi, S.A., Mohajjel, M., Lacombe, O., 2009. New constraints on deformation history of the Zagros hinterland: evidences from calcite twin morphology and geothermometery in sargaz complex, sanandaj-sirjan zone, SE Iran. J. Sci. Islam. Repub. Iran 20 (2), 127–138.
Shafiei, S.H., Alavi, S.A., Mohajjel, M., 2011. Calcite twinning constraints on paleostress patterns and tectonic evolution of the Zagros hinterland: the Sargaz complex, Sanandaj–Sirjan zone, SE Iran. Arab. J. Geosci. 4, 1189–1205. https://doi.org/10.1007/s12517-010-0140-3.
Sieh, K., Jones, L., Hauksson, E., Hudnut, K., Eberhart- Phillips, D., Heaton, T., Hough, S., Hutton, K., Kanamori, H., Lilje, A., Lindvall, S., McGill, S.F., Mori, J., Rubin, C., Spotila, J.A., Stock, J., Thio, H.K., Treiman, J., Wernicke, B., Zachariasen, J., 1993. Near-field investigations of the Landers earthquake sequence, april to july 1992. Science 260, 171–176.
Stein, S.R., Barka, A.A., Dieterich, J.H., 1997. Progressive failure on the North Anatolian fault since 1939 by earthquake stress triggering. Geophys. J. Int. 128, 594–604.
Stocklin, J., 1974. Possible ancient continental margin in Iran. In: Burk, C.A., Drake, C.L. (Eds.), The Geology of Continental Margins. Springer, Berlin, pp. 873–887.
Takin, M., 1972. Iranian geology and continental drift in the Middle East. Nature 235 (5334), 147–150.
Talebian, M., Jackson, J., 2002. Offset on the main recent fault of NW Iran and implications for the late cenozoic tectonics of the arabia-eurasia collisionzone, geophys. J. Intell. 150, 422–439.
Talebian, M., Fielding, E.J., Funning, G.H., Ghorashi, M., Jackson, J., Nazari, H., Parsons, B., Priestley, K., Rosen, P.A., Walker, R., Wrigh, T.J., 2004. The 2003 Bam (Iran) earthquake: rupture of a blind strike-slip fault. Geophys. Res. Lett. 31, L11611. https://doi.org/10.1029/2004GL020058, 2004.
Tatar, M., Hatzfeld, D., Moradi, A.S., Paul, A., 2005. The 2003 December 26 Bam earthquake (Iran), M 6.6, aftershock sequence. Geophys. J. Int. 163, 90–105.
Vavryčuk, V., Adamová, P., 2018. Detection of stress anomaly produced by interaction of compressive fault steps in the West Bohemia swarm region, Czech Republic. Tectonics 37, 4212–4225. https://doi.org/10.1029/2018TC005163.
Vernant, P., et al., 2004. Present-day crustal deformation and plate kinematics in the Middle East constrained by GPS measurements in Iran and northern Oman, Geophys. J. Intell. 157, 381–398.
Walker, R., Jackson, J., 2002. Offset and evolution of the Gowk fault, S.E. Iran: a major intra-continental strike-slip system. J. Struct. Geol. 24, 1677–1698.
Walker, R., Jackson, J., 2004. Active tectonics and late Cenozoic strain distribution in central and eastern Iran. Tectonics 23 (5), TC5010.
Walker, R.T., Priestley, K., Andalibi, M.J., Gheitanchi, M.R., Jackson, J.A., Karegar, S., 2005. Seismological and field observations from the 1990 November 6 Furg (Darabe Hormozgan) earthquake: a rare case of surface rupture in the Zagros mountains of Iran. Geophys. J. Int. 163, 567–579.
Walker, R.T., Gans, P., Allen, M.B., Jackson, J., Khatib, M., Marsh, N., Zarrinkoub, M., 2009. Late Cenozoic volcanism and rates of active faulting in eastern Iran. Geophys. J. Int. 177, 783–805.
Walker, R.T., Bergman, E.A., Szeliga, W., Fielding, E.J., 2011. Insights into the 1968-1997 Dasht-e- Bayaz and Zirkuh earthquake sequences, eastern Iran, from calibrated relocations, InSAR and high- resolution satellite imagery. Geophys. J. Int. 187, 1577–1603.
Walker, R.T., Bergman, E.A., Elliott, J.R., Fielding, E.J., Ghods, A.R., Ghoraishi, M., Jackson, J., Nazari, H., Nemati, M., Oveisi, B., Talebian, M., Walters, R.J., 2013. The 2010–2011 South Rigan (Baluchestan) earthquake sequence and its implications for distributed deformation and earthquake hazard in southeast Iran. Geophys. J. Int. 193 (1), 349–374. https://doi.org/10.1093/gji/ggs109.
Walsh, J.J., Watterson, J., Bailey, W.R., Childs, C., 1999. Fault relays, bends and branch-lines. J. Struct. Geol. 21, 1019–1026.
Wilcox, R.E., Harding, T.P., Seely, D.R., 1973. Basic wrench tectonics. AAPG (Am. Assoc. Pet. Geol.) Bull. 57, 74–96.
Woodcock, N.H., Fischer, M., 1986. Strike-slip duplexes. J. Struct. Geol. 8, 725–735.
Yamamoto, Y., Takahashi, N., Pinar, A., Kalafat, D., Citak, S., Comoglu, M., Polat, R., Kaneda, Y., 2017. Geometry and segmentation of the North Anatolian Fault beneath the Marmara Sea, Turkey, deduced from long-term ocean bottom seismographic observations. J. Geophys. Res.: Solid Earth 122, 2069–2084. https://doi.org/10.1002/2016JB013608. J. Geophys.Res. Solid Earth.
Yamini-Fard, F., 2003. Sismotectonique et structure lithosphérique de deux zones de transition dans le Zagros (Iran): la zone de Minab et la zone de Qatar-Kazerun. Université J. Fourier - Grenoble I, France.
Yamini-Fard, F., Hatzfeld, D., Farahbod, A.M., Paul, A., Mokhtari, M., 2007. The diffuse transition between the Zagros continental collision and the Makran oceanic subduction (Iran): microearthquake seismicity and crustal structure. Geophys. J. Int. 170, 182–194.
Zarifi, Z., Nilfouroushan, F., Raeesi, M., 2014. Crustal stress map of Iran: insight from seismic and geodetic computations. Pure Appl. Geophys. 171, 1219–1236.